

GLOBAL ANALOGUE OF THE AHARONOV-BOHM EFFECT

Thesis by

Robert Navin

In Partial Fulfillment of the Requirements

for the Degree of

Doctor of Philosophy

California Institute of Technology

Pasadena, California

1993

(Submitted 17th. April, 1993)

© 1993

Robert Navin

All Rights Reserved

Acknowledgments

I would like to thank my advisor Professor John Preskill for very many discussions. I would also like to thank Professor John Schwarz under whose supervision I took the Caltech doctoral candidacy oral exam in closed string field theory.

Discussions with Patrick McGraw were useful and Ho-Kwong Lo pointed out some errors in a preliminary draft of the manuscript.

I would also like to acknowledge the influence of the encouraging and inspiring Physics teachers that I have had since first studying the subject: my high school teacher, Yvonne Mabbutt B.Sc.; my tutor, Professor Alan Watson, and my project supervisor, Professor Jim Morgan of the Physics Department at the University of Leeds; Dr. I. Boyle of the Mathematics Department at the University of Leeds; Drs. J. Stewart and M. Perry of the Department of Applied Mathematics and Theoretical Physics at the University of Cambridge, whose courses, on General Relativity and Black Holes, I enjoyed the most of the Part III studies; Dr. G. West of the Particle Physics group at the Los Alamos National Laboratory (whose influence led me to renounce string theory!), and finally the other Physics students from whom I have benefitted the most by studying with and discussing Physics, Richard Braganza at Leeds, Duncan Curtis at Cambridge, Christof Schmidhuber, Martin Bucher and Gunnar Klinkhammer at Caltech.

I would also like to thank my parents, Barbara and Brian, for their love and support.

Abstract

This thesis deals with a global analogue of the Aharonov-Bohm effect previously pointed out by other authors. The effect was not well understood because the pure Aharonov-Bohm cross section was thought to be merely an approximate low energy limit. This thesis provides a detailed analysis and reveals that in the particular model considered, there is an exact Aharonov-Bohm cross section over the energy range that a mass splitting occurs. At energies slightly above the mass splitting, the effect has completely disappeared and there is effectively no scattering at large distances. This is a curious observation as it was previously thought that a global theory would not act exactly like a local one over an extended range of energies. It begs the heretical speculation that experimentally observed forces modelled with Lagrangians possessing local symmetries may have an underlying global theory.

Table Of Contents

| | |
|---|---------|
| Chapter 1. Introduction | Page 1 |
| Chapter 2. Scattering Off Global Monopoles | Page 13 |
| Chapter 3. Scattering Off Global Vortices: Off-Diagonal Contribution | Page 23 |
| Chapter 4. Conclusions and Discussion | Page 63 |

*To Lene Toft:
in imperfection
there is beauty,
and pain.*

1. Introduction.

The great triumph of particle physics is the discovery that nature possesses certain exact symmetries even though, experimentally, they are not immediately apparent.

The idea itself is an old one—a simple example is the ferromagnet. An initial analysis might lead one to believe that the direction of magnetisation has some physical significance and thus the laws are not rotationally invariant. This is not the case, of course, and can be seen in a variety of ways: study the system microscopically to find that the magnetic domains choose a random direction but interactions determine whether they favour being lined up, or heat up the magnet and discover that the rotational, $O(3)$ symmetry is restored from its broken symmetry state of rotations only about the magnetisation axis, $U(1)$. The order parameter, *i.e.*, magnetisation M , has condensed in the low temperature phase and is in the symmetric state in the high temperature phase.

The Landau-Ginzburg^[1] theory expresses these ideas neatly^{*}. Near the temperature where the transition between a phase of spontaneous magnetisation and none occurs (the Curie temperature, T_C), the magnetisation \mathbf{M} , is expected to only take small values. Consider an expansion of the free energy U , in \mathbf{M} :

$$U(\mathbf{M}) = (\partial_i \mathbf{M})^2 + \alpha_1(T)(\mathbf{M} \cdot \mathbf{M}) + \alpha_2(\mathbf{M} \cdot \mathbf{M})^2, \quad (1.1)$$

where all terms are rotationally ($O(3)$) symmetric and slowly varying values of \mathbf{M} are assumed to be the field configurations of lowest energy. At the Curie point α_1 vanishes

$$\alpha_1 = \alpha(T - T_C) \quad (1.2)$$

and so the next highest order term is also included. The ground state minimises the

^{*} The following summary is taken from the excellent book by Cheng and Li.^[2]

free energy and so

$$\mathbf{M}[\alpha_1 + 2\alpha_2(\mathbf{M} \cdot \mathbf{M})] = 0. \quad (1.3)$$

For $T > T_C$, the magnetisation is zero and for $T < T_C$ the zero value is a maxima of the free energy, and the lowest value satisfies

$$|\mathbf{M}| = \sqrt{\frac{-\alpha_1}{2\alpha_2}}, \quad (1.4)$$

and so the direction is arbitrary. The system's random choice of magnetisation direction, as the temperature is lowered, spontaneously breaks the full rotational symmetry to that of rotations about the magnetisation axis.

The Landau-Ginzburg theory is an example of the global symmetry group $O(3)$ being spontaneously broken to $U(1)$. The hidden symmetry group present in the electroweak sector of the standard model $SU(2) \otimes U(1)$, is local rather than global but is broken analogously at low temperature to the familiar exact local $U(1)$ invariance of Quantum Electrodynamics. The beautiful illustration of the 'hiddenness' of the symmetry is the fact that the full symmetry group allows neither the electron nor any other fermion, a mass, just as the magnet cannot have a preferred direction of magnetisation in a rotationally invariant theory, but the condensing of an order parameter, the Higgs field, via the Higgs mechanism^[3] allows the electrons to be effectively massive at low energies.

New experimental opportunities to work with spontaneously broken global symmetries have become apparent with liquid crystals^[4] which have elongated molecules causing long range correlations to become prevalent below a phase transition, typically near room temperature, whilst at high temperature the symmetry is restored.

Spontaneously broken symmetries lead to a variety of interesting effects. If the order parameter has a choice of values that lie in a manifold of non-trivial topology such as the two sphere for the (maximal) magnetisation of the ferromagnet, defects may form at the phase transition and persist in the broken symmetry phase. An example in the above case is a solid spherical ferromagnet with the entire surface

a North (such a configuration is not, of course, possible unless magnetic monopoles exist and have a non-zero charge density somewhere inside). Defects may be classified by the homotopy groups of the vacuum manifold (*e.g.*, see the review article by Mermin^[5]). For a full symmetry group G broken to a subgroup H , the homotopy groups of interest are $\pi_n(G/H)$ [†] and for the above case $O(3) \rightarrow U(1)$,

$$\pi_2(O(3)/U(1)) \approx \pi_2(S^2) \approx Z,$$

and this classifies the integer windings that are possible for such a defect.

If fields are coupled to the order parameter, as is the case for the standard model, there is an even wider variety of phenomena. The Higgs mechanism of mass generation is one example. Consider the situation at energies below excitations of the order parameter so that its quantum effects may be ignored and the vacuum expectation value (*vev*) treated as a classical field. At each point in space the Hamiltonian is dependent on the value of the order parameter. Changing position in the vicinity of a defect then is like varying the value of the Hamiltonian, at least for adiabatic transport. This brings the last underlying theme of this thesis to the fore—Berry’s phase^{[7][8]}.

For adiabatic variation of an Hamiltonian’s parameters, an energy eigenstate will remain an energy eigenstate according to the adiabatic theorem (*e.g.*, see Messiah^[9]), but in addition to the expected phase change due to the eigenstate’s energy changing, there is a geometric phase change occurring[‡]. For a Schrödinger equation with a parameterised Hamiltonian $H(\lambda)$ with an isolated energy eigenstate of energy $E(\lambda)$, then the solution of the time dependent Schrödinger equation

$$i \frac{d\psi_T(s)}{ds} = H(s/T)\psi_T(s) \tag{1.5}$$

† It has recently been realised that defects may be energetically stable, typically for a limited range of parameters of the theory, even though the corresponding vacuum manifold’s homotopy classes are trivial^[6].

‡ The following summary is taken from B. Simon’s paper^[8] on the connection between Berry’s phase and the holonomy in an Hermitian line bundle.

has the property that for $T = 0$, $\psi_T(0) = \phi_0$, an eigenvector of $H(0)$,

$$H(0)\psi_0 = E(0)\psi_0, \quad (1.6)$$

and as $T \rightarrow \infty$, $\psi_T(T)$ approaches the eigenvector ϕ_1 of $H(1)$:

$$H(1)\phi_1 = E(1)\phi_1. \quad (1.7)$$

The surprise is that under adiabatic transport round a closed curve C , in parameter space, the overall phase change (for a phase change is all that occurs) is not the naive guess

$$\phi_1 = \exp \left[-i \int_0^T E(s/T) ds \right] \phi_0 \quad (1.8)$$

but

$$\phi_1 = \exp \left[-i \int_0^T E(s/T) ds \right] \exp[i\gamma(C)]\phi_0, \quad (1.9)$$

where $\gamma(C)$ is an extra phase. This phase factor is the solid angle subtended by the closed path at the point that a degeneracy, of the state transported with some other, occurs. The same is true of a closed line integral of the magnetic vector potential around a magnetic monopole and so, in this sense, the degeneracies have a magnetic monopole like property. If the degeneracies occur over an extended region of the parameter space, then for transport in that region, the $U(1)$ connection (of a monopole) is replaced by a $U(N)$ monopole connection^[10].

The synthesis of these ideas lead to the papers on “Adiabatic Effective Lagrangians” by Moody, Shapere, and Wilczek^[11] which fully clarified the previous somewhat mysterious isolated examples of the properties of electron wavefunctions in the presence of Nuclei[§]. The variable parameters of the Hamiltonian being the orientation of the nucleus and its electric dipole moment and the adiabatic limit being the

§ *e.g.*, Longuet-Higgins^[12] and Stone^[13] discussed the sign changes of electron wavefunctions under adiabatic transport around degeneracies.

neglect of the kinetic term of the nucleus. This point is returned to in the concluding remarks of chapter 4.

The possibility of a global analogue of the Aharonov-Bohm effect^[14] became apparent to March-Russell, Preskill, and Wilczek^[15] for a complex scalar coupled to a condensed order parameter will be given a mass term from the coupling[¶]. Consider a theory in a universality class of the following Lagrangian

$$\mathcal{L} = |\partial\lambda|^2 + |\partial\eta|^2 + m^2|\eta|^2 + g(\lambda\eta^2 + \text{h.c.}), \quad (1.10)$$

which enjoys the following global symmetry for the two complex scalars λ and η ,

$$\begin{aligned} \lambda &\rightarrow e^{i\theta(x)}\lambda, \\ \eta &\rightarrow e^{-i\theta(x)/2}\eta. \end{aligned} \quad (1.11)$$

If the field λ condenses $\langle\lambda\rangle = v$, then the couplings effect at lowest energy is a mass splitting. For instance if v is real and $\eta = \eta_1 + i\eta_2$ for η_1, η_2 real, the coupling looks like

$$\Delta\mathcal{L} = gv(\eta_1^2 - \eta_2^2) : \quad (1.12)$$

it is causing a mass splitting between the real and imaginary parts of η .

Two possible experimental realisations of this system can be imagined, they are in nematic liquid crystals and superfluids. The liquid crystal experiment would have to be a mix of two different liquids, one of which condenses and the other does not. The coupling between the two would have to be weaker than the self-coupling and sensitive to the orientation of *one* of the molecules, but not the other, to give the different global charges that are required. The second realisation is outlined by Khazan^[16] in the ‘A’ phase of superfluid Helium; He³-A. The order parameter (λ) is the orientation of the Cooper pairs of Helium atoms. The coupled field (η) is the wavefunction for the

¶ Khazan^[16] noted some years earlier the possibility of such a dynamical system in the ‘A’ phase of He³.

(small) probability amplitude that the Cooper pairs of Helium atoms line up in the reverse direction to the most probable direction (the order parameter). If the order parameter (the vacuum of the Cooper pairs' wavefunction) has a “spin-orbital angular momentum state”

$$|s, s_m\rangle \otimes |l, m\rangle = |1, 0\rangle \otimes |1, 1\rangle, \quad (1.13)$$

(He³-A by definition) then the coupled field η is the orbital angular momentum

$$|l, m\rangle = |1, -1\rangle, \quad (1.14)$$

part of the wavefunction. The coupling is equivalent to global charges of one and half respectively, because under transport round a closed curve the two have different boundary conditions. The Cooper pair spin vector (or “d-vector”) may be rotated by only π and this may be continuous (when combined with rotations by π of the orbital angular momentum part), whereas, the excitation η (or “clapping-mode”) must be rotated by 2π to be continuous under transport round a closed curve. More detail is given in the very readable review of Salomaa and Volovik^[17].

The local mass eigenstates, ρ_i say, may be found in the vicinity of a global vortex

$$\langle \lambda \rangle = v e^{i\phi} \quad (1.15)$$

where ϕ is the azimuthal angle around the vortex, but as the global charge of the two is different, then adiabatic transport around a global vortex will be associated with incomplete rotation of the local mass eigenstate basis, “frame dragging,” that will lead to a phase change of π under transport around the vortex:

$$\rho_i(\phi + 2\pi) = -\rho_i(\phi). \quad (1.16)$$

The Berry's phase parameters are spatial: the $v\eta$ of the condensed field λ . Scattering at the lowest energies will correspond to the mass eigenstate basis being important: an adiabatic condition. The sign change of the mass eigenstates under transport round a closed curve will cause a maximal Aharonov-Bohm effect.

Some debate has, however, arisen over this issue. Namely, does the low energy limit give rise to exactly the Aharonov-Bohm effect or are there corrections and at what energy does the Aharonov-Bohm effect disappear? The frame dragging gives rise to an effective local gauge field, or connection (occurring in the kinetic term of the scattered field), that is just the rotation from the global charge eigenstates to the mass eigenstates. If the mass eigenstates are ρ_1 and ρ_2 then there exists a local, transformation $U(x)$, from the basis η, η^* to this basis: the connection

$$\begin{pmatrix} \rho_1 \\ \rho_2 \end{pmatrix} = U(x) \begin{pmatrix} \eta \\ \eta^* \end{pmatrix} = \frac{1}{\sqrt{2}} \begin{pmatrix} e^{i\phi/2} & e^{-i\phi/2} \\ -ie^{i\phi/2} & ie^{-i\phi/2} \end{pmatrix} \begin{pmatrix} \eta \\ \eta^* \end{pmatrix}. \quad (1.17)$$

The full kinetic term becomes

$$|\partial_i \eta|^2 \rightarrow |(\partial_i + iA_i)\rho|^2, \quad (1.18)$$

where $A_i = i\partial_i U(x)U(x)^\dagger$. For this set up there is only a ϕ component; it is

$$U^\dagger \partial_\phi \eta = \left(\partial_\phi + \frac{1}{2}i\sigma_2 \right) \rho. \quad (1.19)$$

This effective local gauge field is off-diagonal in the Hamiltonian and it is not immediately clear that its effect will exactly reproduce the Aharonov-Bohm effect.

The calculation of March-Russell *et al.*^[15] is significant in this respect as they attempt an explicit calculation of the scattering in the formalism of this dragged frame with its ‘fictitious centrifugal’ connection (fictitious in the sense of the usual centrifugal force—it is a figment of the accelerated observer’s imagination) and they find corrections to the Aharonov-Bohm effect, that is they go beyond Berry’s phase and find more corrections to the adiabatically transported state in addition to Berry’s phase.

The method is simple. The Schrödinger equation satisfied by the mass eigenstates

is

$$-\partial_t^2 \begin{pmatrix} \rho_1 \\ \rho_2 \end{pmatrix} = \begin{pmatrix} [-\nabla^2 + \frac{1}{4r^2} + \mu_1^2] & -\frac{\partial_\phi}{r^2} \\ \frac{\partial_\phi}{r^2} & [-\nabla^2 + \frac{1}{4r^2} + \mu_2^2] \end{pmatrix} \begin{pmatrix} \rho_1 \\ \rho_2 \end{pmatrix} \quad (1.20)$$

together with the boundary condition $\rho_i(\phi + 2\pi) = -\rho_i(\phi)$, where the perturbed masses are $\mu_{(1,2)}^2 = m^2 \pm \Gamma$. Consider an energy and angular momentum eigenstate

$$\psi_n = e^{-i\omega t} e^{i(n+\frac{1}{2})\phi} u(r). \quad (1.21)$$

Drop the off-diagonal terms. The remaining part of the centrifugal potential is its square $1/4r^2$. This causes a small finite correction to the divergent Aharonov-Bohm cross section which is caused by the “exotic” fractional values of angular momentum. The result, in terms of the scattering angle $\theta = \pi - \phi$, is

$$\sigma(\theta) = \frac{1}{2\pi k_2} \frac{1}{\sin^2(\theta/2)} [1 + C(\theta)], \quad (1.22)$$

where the maximum value of $C(\theta)$ is 0.202 at $\theta = \pi$. The expectation of March-Russell *et al.* is that this effect is the correct low energy limit and that it will go away at high energies due to more corrections appearing as the scattering energy is increased. The small expansion parameter is $k_2^4/2\Gamma^2$, the ratio of the momentum to mass splitting. This shows up as a prefactor of all partial waves in a calculation at second order in perturbation theory. The physical reason is that the Berry’s phase Aharonov-Bohm cross section is only valid in the adiabatic limit, *i.e.*, zero momentum. As the momentum is increased, the effective local gauge field will come into effect and cancel off the Aharonov-Bohm effect. This “strong” effect that the effective gauge field has is reflected in the fact that it has a low momentum limit that is non-trivial, a small correction to the Aharonov-Bohm cross section itself.

On the other hand the considerations of Berry would indicate that the form of the connection is purely due to the ‘degeneracy’ at some point inside the vortex core where the full symmetry is restored and the mass splitting is zero. This indicates a pure Aharonov-Bohm effect. This argument seems very weak though, as Berry’s

phase explicitly talks about the parameters being non-spatial, and the confusion we have is that the parameters turn up in the gradient operators. Any changes of basis that we perform produces effective local connections in the momentum operator, not a situation seen in the usual expressions of Berry's phase. But A. Goldhaber^[18] outlines the following two arguments.

The first is about the nature of the adiabatic limit. We take expectation values of the Hamiltonian to get an adiabatic effective Hamiltonian. We did this with the λ field, replaced it by its *vev* instead of solving the full quantum mechanical theory and solved this new theory assuming it will be the low energy limit of the full theory^{*}. This may be the case with the momentum operator. Take only its on-diagonal part in the adiabatic limit, and this knocks off all of the centrifugal potential because it is all off-diagonal leaving a pure Aharonov-Bohm effect.

Secondly, this planar motion is the equivalent of the monopole type considerations in three dimensions elucidated in the papers by Moody *et al.*^[11] describing adiabatic effective Lagrangians. They maintain that the connection is pure magnetic monopole, and the scattering is just that of a charged scalar off a magnetic monopole. The planar equivalent of this is merely the boundary condition on the wavefunction, just the maximal scattering of a charged scalar off a magnetic vortex—the maximal Aharonov-Bohm effect.

It is to this current status that the following thesis makes a contribution. As an interesting review of the vortex calculation of March-Russell *et al.*, the generalisation to the monopole case is presented in chapter 2 to underscore the broadness of the ideas behind the calculation. The 'same' effect is found, the on-diagonal part of the effective local connection is found to be exactly that for a charged scalar on a monopole background, which is the equivalent of the boundary condition on the mass

* 'Low energy' in this context meaning energies well below the effect of the lowest excitation energies of the λ field. Of course, the Goldstone bosons are massless and so they may have an effect. However, they are derivatively coupled and so their effect, on elastic scattering, is suppressed by $(k_2/F)^2$ where F is the symmetry breaking scale. They will not wash out the generic effect that we are discussing.

eigenstate in the vortex case. The off-diagonal parts square up to a $1/4r^2$ additional potential, which is the only on-diagonal modification to the monopole-charged scalar problem that the global case provides.

The main results are presented in chapter 3 where the vortex case is returned to and a calculation of the full coupled relativistic problem (without dropping the off-diagonal terms) is presented and the scattering is found to be pure Aharonov-Bohm. The complicated off-diagonal local effective connection field has an overall effect of zero on the scattering of the mass eigenstates; it is reminiscent of a transmission effect, the parameters are finely tuned to have no overall effect. A metaphor would be the calculation of the trajectory of an object (in Newtonian physics) in a rotating frame. Correct inclusion of all fictitious forces conspires to allow a transformation to a frame in which the calculation vastly simplifies, indicating that some fundamental simplification could have been made initially, but was missed.

The full calculation of the coupled problem in the global monopole case would presumably again find a result similar to the full vortex solution—the effective gauge correction/connection field will give the same scattering cross section as a charged scalar in a monopole field.

Thus, this thesis brings into sharp focus the rôle that effective connections play in systems of fields coupled to condensed order parameters with global defects.

REFERENCES

1. V. L. Ginzburg and L. D. Landau, *J. expl. theoret. Phys. USSR.* **20**, 1064 (1950).
2. T-P. Cheng and L-F. Li, “*Gauge Theory of Elementary Particle Physics*,” Oxford University Press, (1984).
3. P. W. Higgs, *Phys. Lett.* **12**, 132 (1964);
P. W. Higgs, *Phys. Rev. Lett.* **13**, 508 (1964).
4. M. J. Bowick, L. Chandar, and E. A. Schiff, “*Cosmological Kibble Mechanism in the Laboratory: String formation in Liquid crystals*,” Syracuse University Preprint, SU-HEP-4241-512;
I. Chuang, N. Turok and B. Yurke, *Phys. Rev. Lett.* **66**, 2472 (1991).
5. N. Mermin, *Rev. Mod. Phys.* **51**, 591 (1979).
6. T. Vachaspati and A. Achúcarro, *Phys. Rev.* **D44**, 3067 (1991);
P. Hindmarsh, *Nucl. Phys.* **B392**, 461, (1993).
7. M. V. Berry, *Proc. R. Soc. Lond.* **A.392**, 45 (1984).
8. B. Simon, *Phys. Rev. Lett.* **51**, 2167 (1983).
9. A. Messiah, “*Quantum Mechanics*,” Vol. 2, Amsterdam: North-Holland (1962).
10. F. Wilczek and A. Zee, *Phys. Rev. Lett.* **52**, 2111 (1984).
11. J. Moody, A. Shapere, and F. Wilczek, *Phys. Rev. Lett.* **52**, 2111 (1984);
J. Moody, A. Shapere, and F. Wilczek, “*Geometric Phases in Physics*,” pp 160–183, Eds. A. Shapere and F. Wilczek, Singapore: World Scientific (1989).
12. H. C. Longuet-Higgins, *Proc. R. Soc. Lond.* **A 344**, 147 (1975).
13. A. J. Stone, *Proc. R. Soc. Lond.* **A 351**, 141 (1976).
14. Y. Aharonov and D. Bohm, *Phys. Rev.* **115**, 485 (1959).
15. J. March-Russell, J. Preskill, and F. Wilczek, *Phys. Rev. Lett.* **68**, 2567 (1992).

16. M. V. Khazan, *Pis'ma Zh. Eksp. Teor. Fiz.* **41**, 396 (1985).
17. M. M. Salomaa and G. E. Volovik, *Rev. Mod. Phys.* **59**, 533 (1987).
18. A. Goldhaber, private communications with J. Preskill.

2. Scattering off Global monopoles: Similarity to Charge-Magnetic Monopole Scattering.

2.1 INTRODUCTION

March-Russell, Preskill, and Wilczek^[1] have demonstrated that a global analogue of the Aharonov-Bohm effect may arise (in an essentially classical context) and further that the cross section for scattering off a global vortex (i.e., a string) may give rise to a cross section of the Aharonov-Bohm form with small corrections.

Specifically, they consider two complex scalar fields, λ and η , say, with a real coupling g ,

$$\Delta\mathcal{L} = g\lambda\eta^2 + h.c. \quad (2.1)$$

If the λ field then condenses, vortices in 2+1 or strings in 3+1 are expected. The coupling causes a mass splitting between the two components of η . The orientation of these components changes around the vortex: frame dragging. Writing the field in terms of these mass eigenstates, ρ_1 and ρ_2 , say

$$\begin{pmatrix} \rho_1 \\ \rho_2 \end{pmatrix} = \frac{1}{\sqrt{2}} \begin{pmatrix} e^{i\phi/2} & e^{-i\phi/2} \\ -ie^{i\phi/2} & ie^{-i\phi/2} \end{pmatrix} \begin{pmatrix} \eta \\ \eta^* \end{pmatrix}, \quad (2.2)$$

it is found that the mass eigenstates have a sign change under rotation by 2π ;

$$\rho_i(\phi + 2\pi) = -\rho_i(\phi).$$

This leads to a cross section for scattering of excitations of the ρ field off the vortex to be of Aharonov-Bohm form. Rewriting the kinetic term in ρ and dropping off diagonal terms that couple the two mass eigenstates gives an “ A^2 ” induced potential term:

$$V_{A^2} = \frac{1}{4r^2}, \quad (2.3)$$

and this leads to a small modification of the Aharonov-Bohm type scattering which was calculated by March-Russell, Preskill, and Wilczek^[1]. The correction potential

was found to give a small alteration to the leading term of maximal Aharonov-Bohm form:

$$\sigma(\theta) = \frac{1}{2\pi k_2} \frac{1}{\sin^2(\theta/2)} [1 + C(\theta)], \quad (2.4)$$

for incident excitation of wavenumber k_2 scattered through angle θ . The off-diagonal terms contribution is suppressed at low momenta.

As $\Gamma \rightarrow 0$, or at high momenta, the effect must go away for finite $\theta > \sqrt{\Gamma}/k$: at large momentum transfer the induced gauge field ‘cancels’ the effect of the modified boundary conditions.

It is natural to then ask about the generalisation to scattering off global monopoles and its relation to scattering by charged scalars off magnetic monopoles. It is this question which is answered here. Specifically, a model with a global $O(3)$ symmetry is broken down to $U(1)$, and global monopoles result. The order parameter is coupled to a complex doublet in such a way that the analogue of frame dragging occurs. A situation closely analogous to the scattering off a vortex case of March-Russell, Preskill, and Wilczek^[1] is found. The on-diagonal parts of the effective connection reproduce the magnetic monopole potential exactly plus a correction potential of the same form, $1/2r^2$, as the vortex case. The cross section is then calculated, and corrections are found to occur at subleading order in the divergent cross section as the forward scattering angle is approached.

Section 2.2 reviews the scattering of charged scalars off a magnetic monopole. The leading divergences in the sum are calculated. The global monopole scattering problem is set up in section 2.3, and its close analogy to the magnetic monopole scattering problem is demonstrated. The formal solution and its expansion follow immediately. Conclusions are drawn in section 2.4.

2.2 SCATTERING OF CHARGED SCALARS BY DIRAC MONOPOLES.

Formal Expression for Scattering Cross Section. The Klein-Gordon (KG) equation (or the Schrödinger equation) of a particle of charge Ze in the presence of a Dirac monopole,

$$-(\nabla + iZe\mathbf{A})^2 \psi = E\psi, \quad (2.5)$$

where in spherical co-ordinates (r, θ, ϕ) ,

$$Ze\mathbf{A} = \begin{cases} -q \frac{(\cos\theta-1)}{r \sin\theta} \hat{\phi} & \text{for } \theta \in R_a : \theta \neq \pi; \\ -q \frac{(\cos\theta+1)}{r \sin\theta} \hat{\phi} & \text{for } \theta \in R_b : \theta \neq 0, \end{cases} \quad (2.6)$$

was first solved by Tamm^[2] in terms of what are now called monopole harmonics^[3]: ${}^q Y_{l,m}(\theta, \phi)$, where the angular momentum quantum number l is greater than or equal to $|q|$ and as usual m runs from $-l$ to l in integer steps. The monopole strength $q = \frac{1}{2}(2eg)Z$ must be half integral (Z and $2eg$ are integers) in order that the wave function be single valued everywhere (Dirac's quantisation condition) up to local gauge transformations, *i.e.*, viewed as a *section*^[3]. Assume, without loss of generality, that q is positive.

A partial wave expansion led Banderet^[4] to an expression for the scattering amplitude $f(\theta)$. I describe the main points of his derivation here as they are central to the global monopole calculation below. The wave equation is solved by energy eigenstates of the form

$$\psi = j_{\nu_l}(kr) {}^q Y_{l,m}(\theta, \phi) \quad (2.7)$$

where $j_{\nu_l}(kr)$ are spherical Bessel functions of order ν_l ,

$$\nu_l = \sqrt{(l + 1/2)^2 - q^2} - 1/2. \quad (2.8)$$

For $q = 0$ we see, as expected, integer order spherical Bessel functions. Writing an

arbitrary energy eigenstate as

$$\psi_k = \sum_{l,m} a_{lm} j_{\nu_l}(kr)^q Y_{l,m}(\theta, \phi) \quad (2.9)$$

we want to match to an incoming wave travelling down the z -axis and then pick out the radially outgoing part of this solution. Banderet was forced to consider an incoming wave of the form $4\pi e^{-ikz} \delta(1 - \cos \theta)$ where the normalisation $\oint d\Omega \delta(1 - \cos \theta) = 1$ is chosen. This is because the monopole harmonics are complete only over angular functions which have a zero. Thus it is not possible to ask the question, how is a wave e^{-ikz} scattered by a magnetic monopole because such a wave will not propagate on a monopole background. This is not a serious problem for scattering as this ‘narrow’ ingoing wave assumption is implicit in the usual derivation of a scattering cross section, *e.g.*, neglecting incoming and outgoing wave interference. This decides the modulus of the a_{lm} coefficients

$$|a_{lm}| = 4\pi^q Y_{l,-q}(\theta = 0). \quad (2.10)$$

In the region (R_a say) including the upper z -axis, but not the lower z -axis, the monopole harmonics of eigenvalue $m = -q$ are ϕ independent and in R_b , the lower region (including the lower z -axis but not the upper), they have ϕ dependence $e^{-i2q\phi}$. The monopole harmonics satisfy a gauge transformation in the overlap region ($R_a \cap R_b$)

$$\psi_a = e^{i2q\phi} \psi_b, \quad (2.11)$$

where ψ_a is the value of the wavefunction in region R_a : this is the definition of a section. Details are discussed at length in the paper on monopole harmonics by Wu and Yang^[3]. The last step is to ensure that the radial dependence of the incoming part of the wave matches to spherical Bessel functions of integer order and hence will

add up to reproduce a plane wave. This determines the phases of the coefficients

$$a_{lm} = 4\pi^q Y_{l,-q}(0) e^{-i\pi\nu_l}. \quad (2.12)$$

The asymptotic form of the wave equation is then picked out and is

$$\psi = 4\pi e^{-ikr \cos\theta} \delta(1 - \cos\theta) + \frac{f(\theta)}{r} e^{ikr} + \dots \quad (2.13)$$

and using $x = \cos\theta$, the scattering amplitude is

$$\begin{aligned} f(\theta) &= \frac{1}{2ik} \sum_l 4\pi e^{-i\pi\nu_l q} Y_{l,-q}(0)^q Y_{l,-q}(\theta) \\ &= \frac{1}{(2ik)} \left(\frac{1+x}{2}\right)^q \sum_{l=q}^{\infty} (2l+1) e^{-i\pi\nu_l} P_{l-q}^{0,2q}(x), \end{aligned} \quad (2.14)$$

using Wu and Yang's^[3] definition of monopole harmonics in terms of Jacobi Polynomials $P_l^{\alpha,\beta}(x)$.

Leading Divergences in the formula of Banderet. The Banderet formula may be approximated by writing ν_l as an expansion in l and noting

$$e^{-i\pi\nu_l} = (-)^l + (-)^l (e^{-i\pi(\nu_l-l)} - 1). \quad (2.15)$$

We find

$$\nu_l - l = \frac{-q^2}{(2l+1)} \sum_{n=0}^{\infty} \frac{2n!}{n!(n+1)!} \left(\frac{q}{2l+1}\right)^{2n}. \quad (2.16)$$

The first few terms of $e^{-i\pi(\nu_l-l)} - 1$ are

$$e^{-i\pi(\nu_l-l)} - 1 = \frac{i\pi q^2}{(2l+1)} - \frac{1}{2} \frac{\pi^2 q^4}{(2l+1)^2} + O\left(\frac{1}{(2l+1)^3}\right). \quad (2.17)$$

The third term will be divergent at $x = -1$, but it will be less divergent as x approaches -1 than the previous two whilst the fourth will be convergent at $x = -1$:

they are not so easily calculated. Using the generating function for Jacobi polynomials

$$\frac{1}{R(1-z+R)^\alpha(1+z+R)^\beta} = \frac{1}{2^{\alpha+\beta}} \sum_{n=0}^{\infty} P_n^{\alpha,\beta}(x) z^n, \quad (2.18)$$

where $R = (1 - 2xz + z^2)^{1/2}$, we know that

$$\begin{aligned} \left(\frac{1+x}{2}\right)^q \sum_{n=0}^{\infty} (-)^n P_n^{0,2q}(x) &= \frac{1}{\sqrt{2(1+x)}} \\ \left(\frac{1+x}{2}\right)^q \sum_{n=0}^{\infty} (-)^n n P_n^{0,2q}(x) &= \frac{1}{\sqrt{2(1+x)}} \left(\frac{1}{2} - q + \sqrt{\frac{2}{1+x}q}\right). \end{aligned} \quad (2.19)$$

Then it follows

$$f(x) = \frac{(-)^q}{(2ik)} \left(\frac{2q}{(1+x)} + \frac{2 + i\pi q^2}{\sqrt{2(1+x)}} + \dots \right). \quad (2.20)$$

For small scattering angles we can see that the main contribution is (coincidentally) from a term of the form of Rutherford scattering. The next correction goes as the sum

$$\left(\frac{1+x}{2}\right)^q \sum_{n=0}^{\infty} \frac{(-)^n}{(n+1/2)} P_n^{0,2q}(x), \quad (2.21)$$

which, as already noted, diverges at $x = -1$. The next term in the series is convergent at $x = -1$.

2.3 SCATTERING OFF A GLOBAL MONOPOLE

Setting up the Problem: Frame Dragging. We couple a real scalar transforming in the fundamental representation of $O(3)$, v^a for $a = 1, 2, 3$, to a complex doublet Φ transforming as the fundamental representation of $SU(2)$, via a term of the form

$$\Delta\mathcal{L} = g\Phi^\dagger\sigma^a\Phi v^a. \quad (2.22)$$

This causes a mass splitting at low energies between the two complex components of the doublet when the real field condenses to $\langle \mathbf{v} \rangle = (0, 0, 1)$. The real field may

condense to form global monopoles. The coupling will still cause a mass splitting and the mass eigenstates will experience frame dragging upon transport around the monopole. We proceed by analogy to the vortex case of March-Russell, Preskill, and Wilczek^[1], by changing variables to the mass eigenstates which gives rise to an induced connection, and we then drop the off-diagonal terms, which couple the mass eigenstates, as these will be suppressed at low momenta.

First, diagonalise the mass matrix perturbation caused by the monopole. We note that

$$U(\Theta)\sigma^3U(\Theta)^\dagger = \frac{r^a}{r}\sigma^a. \quad (2.23)$$

where in spherical polar co-ordinates the vector Θ is $\Theta = \theta\hat{\phi}$, and

$$U(\Theta) = \exp -\frac{i}{2}\Theta \cdot \sigma. \quad (2.24)$$

We change variable from Φ to ρ ,

$$\rho = U(\Theta)^\dagger\Phi, \quad (2.25)$$

and find that the interaction term looks like

$$g\rho^\dagger\sigma^3\rho = \frac{1}{2}\Gamma(|\rho_1|^2 - |\rho_2|^2). \quad (2.26)$$

The important point is that the field has nontrivial transport properties around the global monopole, and indeed there must be a zero in the field configuration somewhere, for the same reasons as were argued in section 2.1 that sections have such a zero. We have transformed to a basis that diagonalises the mass term everywhere around the monopole, and this requires a spatially dependent rotation of axes.

The kinetic term is now written

$$\begin{aligned}\partial_\mu\Phi^\dagger\partial_\mu\Phi &= \left|(\partial_\mu + U^\dagger\partial_\mu U)\rho\right|^2 \\ &= \partial_\mu\rho^\dagger\partial_\mu\rho + \rho^\dagger(\partial_i U^\dagger U)\partial_i\rho + \partial_i\rho^\dagger(U^\dagger\partial_i U)\rho + \rho^\dagger(\partial_i U^\dagger\partial_i U)\rho.\end{aligned}\tag{2.27}$$

Explicitly calculating this, dropping off-diagonal terms only and writing ρ in terms of its complex components $\rho = (\rho_1, \rho_2)$, we find that the kinetic term may be written

$$\partial_\mu\rho_1^\dagger\partial_\mu\rho_1 + \rho_1^\dagger(-iqA_i)\partial_i\rho_1 + \partial_i\rho_1^\dagger(iqA_i)\rho_1 + \rho_1^\dagger\left(\frac{1}{2r^2} + q^2A_i^2\right)\rho_1,\tag{2.28}$$

where qA_i is just a magnetic monopole field in the upper region R_a with $q = \frac{1}{2}$. $A_i = (0, 0, A_\phi)$ where

$$A_\phi = -\frac{(\cos\theta - 1)}{r\sin\theta}.\tag{2.29}$$

The full kinetic term is a sum of the above term and a term in ρ_2 with the opposite magnetic charge $q = -\frac{1}{2}$. The Schrödinger equations for both of the components, in the nonrelativistic limit, may be written

$$\frac{1}{2m_i}\left[-(\nabla + iq\mathbf{A})^2 + \frac{1}{2r^2}\right]\rho_i = E\rho_i,\tag{2.30}$$

where for $i = 1$, $q = \frac{1}{2}$, and for $i = 2$, $q = -\frac{1}{2}$, and the masses differ due to the mass splitting discussed. We see an almost exactly analogous structure to the vortex case. There is the ‘‘Aharonov-Bohm’’ effect, i.e., the monopole potential, and a ‘correction’ potential $1/(2r^2)$.

Scattering Cross Section. The cross section is easily calculable by analogy to the previous calculation by Banderet. The radial part of the separated equation is all that is modified, and so the phase shifts ν_l are modified,

$$\tilde{\nu}_l = \sqrt{(l + 1/2)^2 - q^2 + 1/2 - 1/2},\tag{2.31}$$

by the factor of $1/2$ inside the square root coming from the correction potential. The

formal expression for the cross section is then

$$f(\theta) = \frac{1}{2ik} \sum_l 4\pi e^{-i\pi\tilde{\nu}_l q} Y_{l,-q}(0)^q Y_{l,-q}(\theta). \quad (2.32)$$

This leads to a modification of the cross section only in the second leading divergent term in the cross section. The scattering amplitudes in the global and local monopole cases are

$$\begin{aligned} f_g(x) &= \frac{(-)^q}{(2ik)} \left(\frac{2q}{(1+x)} + \frac{2+i\pi(q^2-1/2)}{\sqrt{2(1+x)}} + \dots \right) \\ f_l(x) &= \frac{(-)^q}{(2ik)} \left(\frac{2q}{(1+x)} + \frac{2+i\pi q^2}{\sqrt{2(1+x)}} + \dots \right), \end{aligned} \quad (2.33)$$

where $q = 1/2$.

2.4 CONCLUSIONS

The situation is closely analogous to the vortex case. The on-diagonal contributions persist at low momenta and reproduce the scattering of scalars off a magnetic monopole with a correction which is subleading for angles closer to the forward direction. The effect is expected to go away for large momenta and the neglected off-diagonal terms give a contribution that may be calculated using perturbation theory. The second order calculation gives terms uniform in all partial waves times k^4/Γ^2 and so it is sensible to predict that the effect goes away for momenta larger than the mass splitting.

The induced connection turned out to be purely that of a monopole on diagonal and the $1/2r^2$ correction potential came from the square of the off-diagonal terms. Dropping the off-diagonal parts in the square of the total gradient term, the remaining correction potential caused a modification of the charged scalar-magnetic monopole scattering cross section only at subleading order in the divergent cross section as the forward scattering angle is approached analogously to the vortex case calculation of March-Russell *et al.*

REFERENCES

1. J. March-Russell, J. Preskill, and F. Wilczek, *Phys. Rev. Lett.* **68**, (1992).
2. I. Tamm, *Z. Phys.* **71**, 141 (1931).
3. T. T. Wu and C. N. Yang, *Nucl. Phys.* **B107**, 365 (1976).
4. P. Banderet, *Helv. Phys. Acta.* **19**, 503 (1946) (in German).

3. Scattering Off Global Vortices: Off-Diagonal Contribution.

3.1 INTRODUCTION.

Given the Lagrangian of equation (1.10)

$$\mathcal{L} = |\partial\lambda|^2 + |\partial\eta|^2 + m^2|\eta|^2 + g(\lambda\eta^2 + \text{h.c.}), \quad (3.1)$$

and putting the value $\lambda = ve^{i\phi}$ in to represent a vortex in the field of the condensed order parameter λ then the local mass eigenstate basis, given by March-Russell, Preskill and Wilczek^[1], is

$$\begin{pmatrix} \rho_1 \\ \rho_2 \end{pmatrix} = \frac{1}{\sqrt{2}} \begin{pmatrix} e^{i\phi/2} & e^{-i\phi/2} \\ -ie^{i\phi/2} & ie^{-i\phi/2} \end{pmatrix} \begin{pmatrix} \eta \\ \eta^* \end{pmatrix}. \quad (3.2)$$

This basis has the odd feature of making the ρ field acquire a minus sign under transport round a closed circle containing the vortex and the kinetic term must be accordingly modified by an effective local connection.

The frame dragged mass eigenstates ρ_i satisfy the following relativistic wave equation

$$-\partial_t^2 \begin{pmatrix} \rho_1 \\ \rho_2 \end{pmatrix} = \begin{pmatrix} [-\nabla^2 + \frac{1}{4r^2} + \mu_1^2] & -\frac{\partial_\phi}{r^2} \\ \frac{\partial_\phi}{r^2} & [-\nabla^2 + \frac{1}{4r^2} + \mu_2^2] \end{pmatrix} \begin{pmatrix} \rho_1 \\ \rho_2 \end{pmatrix} \quad (3.3)$$

together with the boundary condition $\rho_i(\phi + 2\pi) = -\rho_i(\phi)$, where the perturbed masses are $\mu_{(1,2)}^2 = m^2 \pm \Gamma$.

The zero order equation (*i.e.*, off-diagonal terms set to zero) was investigated by March-Russell *et al.*^[1] and a solution constructed out of a complete orthogonal set representing an incoming plane wave and a radially scattered outgoing wave to leading orders in $1/\sqrt{r}$. The leading effect is an Aharonov-Bohm type scattering cross section.

A calculation of the cross section for scattering a plane wave of the full coupled relativistic wave equation, (3.3), is obtained. A pure ρ_2 state is still not expected to excite a real ρ_1 mode as this would not conserve energy. The ρ_2 modes can be affected at second order in the off-diagonal terms corresponding to ‘virtual’ ρ_1 excitation. A calculation at second order in perturbation theory shows that the scattering of the ρ_2 modes falls off with r more strongly than the leading terms, *i.e.*, the incoming and outgoing waves, and so does not affect the cross section. This is a very strange effect to observe. Firstly, a modification to the potential, however weak, should alter the cross section at some order. But more curiously is that in this case we *expect* the Aharonov-Bohm effect to disappear at high momenta and as this is “caused” by the effective potential, we would expect a stronger effect than nothing. As this does not show up at second order in perturbation theory, a full solution to the (relativistic) wave equation would be very illuminating.

It turns out to be possible to calculate the full relativistic solution to the coupled equation. This is now given in terms of modes that look exactly like Bessel functions at large r . There are two possible solutions for each angular momentum eigenfunction. This leads directly to the conclusion that the pure Aharonov-Bohm effect occurs for scattering of a pure plane wave off the vortex.

3.2 FULL COUPLED EQUATION.

Energy and Angular Momentum Eigenfunctions. The wave equation satisfied by ρ is

$$-\partial_t^2 \begin{pmatrix} \rho_1 \\ \rho_2 \end{pmatrix} = \begin{pmatrix} [-\nabla^2 + \frac{1}{4r^2} + \mu_1^2] & -\frac{\partial_\phi}{r^2} \\ \frac{\partial_\phi}{r^2} & [-\nabla^2 + \frac{1}{4r^2} + \mu_2^2] \end{pmatrix} \begin{pmatrix} \rho_1 \\ \rho_2 \end{pmatrix} \quad (3.4)$$

together with the boundary condition $\rho_i(\phi + 2\pi) = -\rho_i(\phi)$. Now looking for a solution of energy eigenvalue ω , $\rho(x, t) = e^{-i\omega t} \rho(r, \phi)$;

$$\begin{aligned} (\omega^2 - L_1)\rho_1 &= -\frac{1}{r^2} \partial_\phi \rho_2 \\ (\omega^2 - L_2)\rho_2 &= \frac{1}{r^2} \partial_\phi \rho_1, \end{aligned} \quad (3.5)$$

where $L_i = -\nabla^2 + \frac{1}{4r^2} + \mu_i^2$, we see that ρ_2 satisfies

$$r^2(\omega^2 - L_1)r^2(\omega^2 - L_2)\rho_2 = -\partial_\phi^2\rho_2. \quad (3.6)$$

The other component, ρ_1 , satisfies the same equation with the subscripts 1 and 2 interchanged everywhere that they appear.

Next, take for ρ_2 the form

$$\rho_2^{(n)} = e^{i(n+\frac{1}{2})\phi} \sum_{k=k_0^{(n)}}^{\infty} b_k^{(n)} r^k, \quad (3.7)$$

which leads immediately to the equation

$$\begin{aligned} \sum_{k=k_0^{(n)}}^{\infty} b_k^{(n)} \left\{ r^{k+4}(\omega^2 - \mu_2^2)(\omega^2 - \mu_1^2) \right. \\ \left. + r^{k+2} \left(([k+2]^2 - \nu_n^2)(\omega^2 - \mu_2^2) + (k^2 - \nu_n^2)(\omega^2 - \mu_1^2) \right) \right. \\ \left. + r^k \left((k^2 - \nu_n^2)^2 - (n + \frac{1}{2})^2 \right) \right\} = 0, \end{aligned} \quad (3.8)$$

where $\nu_n^2 = (n + \frac{1}{2})^2 + \frac{1}{4}$. For non-zero $b_k^{(n)}$, suppressing the n superscript,

$$\begin{aligned} b_{k-2}(\omega^2 - \mu_2^2)(\omega^2 - \mu_1^2) + b_k \left\{ ([k+2]^2 - \nu_n^2)(\omega^2 - \mu_2^2) \right. \\ \left. + (k^2 - \nu_n^2)(\omega^2 - \mu_1^2) \right\} + b_{k+2} \left\{ ([k+2]^2 - \nu_n^2)^2 - (n + \frac{1}{2})^2 \right\} = 0. \end{aligned} \quad (3.9)$$

We follow the process that obtains Bessel functions as a power series. The solution should be finite at the origin, thus a minimum value of k , k_0 say, should truncate the series' descent. Thus $b_{k_0-2} = 0$ implies

$$b_{k_0+2} = -b_{k_0} \frac{\left\{ ([k_0+2]^2 - \nu_n^2)(\omega^2 - \mu_2^2) + (k_0^2 - \nu_n^2)(\omega^2 - \mu_1^2) \right\}}{\left\{ ([k_0+2]^2 - \nu_n^2)^2 - (n + \frac{1}{2})^2 \right\}}, \quad (3.10)$$

and $b_{k_0-4} = 0$ implies

$$(k_0^2 - \nu_n^2)^2 - (n + \frac{1}{2})^2 = 0. \quad (3.11)$$

| n | $k_0^{(-)}$ | $k_0^{(+)}$ |
|----------|-------------|-------------|
| \vdots | \vdots | \vdots |
| -2 | 2 | 1 |
| -1 | 1 | 0 |
| 0 | 0 | 1 |
| 1 | 1 | 2 |
| \vdots | \vdots | \vdots |

Table 1. Values of k_0 .

Spectrum. As k_0 must be greater than -1 , to ensure square-integrability, there are two possibilities for k_0 , $|n|$ and $|n + 1|$, which we label as follows:-

$$k_0^{(+)} = |n + 1|, \quad k_0^{(-)} = |n|, \quad (3.12)$$

i.e.,

$$k_0^{(\pm)2} - \nu_n^2 = \pm(n + \frac{1}{2}). \quad (3.13)$$

The values of k_0 for n near zero are shown in table 1. There is one important point to note. All the angular momentum modes are doubly degenerate with the possible exception of the $n = 0, -1$ modes that are zero at the origin. Note that these modes have angular dependence $\exp \pm i\phi/2$. These modes would have to be excluded to ensure that all the functions are zero at the origin: a constant value is not consistent with the ϕ dependence of all modes or the non-interaction with the vortex core approximation. However, a small r expansion of the finite size core solution allows these modes, and for a wall thickness of zero they are not affected. We shall allow them into the spectrum although, bear in mind, they may probe the vortex core and thus violate the decoupling principle.

Thus, using b_{k_0} the entire series is generated for each angular momentum eigenvalue by the recursion relation

$$b_{k+2} = \frac{b_{k-2}(\omega^2 - \mu_2^2)(\omega^2 - \mu_1^2) + b_k \left\{ ([k+2]^2 - \nu_n^2)(\omega^2 - \mu_2^2) + (k^2 - \nu_n^2)(\omega^2 - \mu_1^2) \right\}}{\left\{ ([k+2]^2 - \nu_n^2)^2 - (n + \frac{1}{2})^2 \right\}}. \quad (3.14)$$

I shall label this function $\tilde{J}_n^{(2,\pm)}(r)$. The normalisation is chosen below so that they go to Bessel functions at large r , for a certain limit of the parameters.

The ρ_1 field may be expanded similarly

$$\rho_1^{(n)} = e^{i(n+\frac{1}{2})\phi} \sum_{k=k'_0}^{\infty} a_k^{(n)} r^k, \quad (3.15)$$

and the recursion relation for its coefficients is the same except that the subscripts 1 and 2 are interchanged everywhere that they appear. The small r expansion of the equation $(\omega^2 - L_2)\rho_2 = (1/r^2)\partial_\phi\rho_1$, shows that $k'_0 = k_0$ and hence

$$b_{k_0}(k_0^2 - \nu_n^2) = i(n + \frac{1}{2})a_{k_0}. \quad (3.16)$$

If the value of a_{k_0} is chosen to be the same for the two solutions, then we find

$$b_{k_0}^{(\pm)} = \pm i a_{k_0}, \quad (3.17)$$

and labelling the ρ_1 solution $\tilde{J}_n^{(1,\pm)}(r)$, we find

$$\rho_n^{(+)} = \begin{pmatrix} \tilde{J}_n^{(1,+)}(r) \\ i\tilde{J}_n^{(2,+)}(r) \end{pmatrix} e^{i(n+\frac{1}{2})\phi}, \quad \rho_n^{(-)} = \begin{pmatrix} \tilde{J}_n^{(1,-)}(r) \\ -i\tilde{J}_n^{(2,-)}(r) \end{pmatrix} e^{i(n+\frac{1}{2})\phi}. \quad (3.18)$$

Large r Behaviour of Solutions. Noting that Bessel function coefficients satisfy the recursion relation

$$a_{k+2} = -\frac{a_k}{[(k+2)^2 - \nu^2]} \quad (3.19)$$

(hence $k_0 = |\nu|$ to truncate the descending series) this type of behaviour can be seen in the recursion relation for the above functions.

$$\begin{aligned} a_{k+2} &= \\ & - \frac{a_{k-2}(\omega^2 - \mu_2^2)(\omega^2 - \mu_1^2) + a_k \left\{ ([k+2]^2 - \nu_n^2)(\omega^2 - \mu_1^2) + (k^2 - \nu_n^2)(\omega^2 - \mu_2^2) \right\}}{\left\{ ([k+2]^2 - \nu_n^2)^2 - (n + \frac{1}{2})^2 \right\}} \\ b_{k+2} &= \\ & - \frac{b_{k-2}(\omega^2 - \mu_2^2)(\omega^2 - \mu_1^2) + b_k \left\{ ([k+2]^2 - \nu_n^2)(\omega^2 - \mu_2^2) + (k^2 - \nu_n^2)(\omega^2 - \mu_1^2) \right\}}{\left\{ ([k+2]^2 - \nu_n^2)^2 - (n + \frac{1}{2})^2 \right\}}. \end{aligned} \quad (3.20)$$

This observation prompts the assumption that the large r behaviour of these modified Bessel functions is $J \sim r^\gamma \cos kr$. Put this into the differential equation

$$\nabla_n^{(\frac{1}{2}, \pm)} J_n^{(\frac{1}{2}, \pm)} = 0 \quad (3.21)$$

where eqn. (3.6) gives ∇_n

$$\begin{aligned} \nabla_n &= \left[r^2(\omega^2 - L_1)r^2(\omega^2 - L_2) - (n + \frac{1}{2})^2 \right] \\ &= r^4(\omega^2 - \mu_1^2)(\omega^2 - \mu_2^2) + r^2 \left\{ 4(\omega^2 - \mu_2^2) - \nu_n^2(2\omega^2 - \mu_1^2 - \mu_2^2) \right\} \\ &\quad + \nu_n^4 - (n + \frac{1}{2})^2 \\ &\quad + \left\{ 1 - 2\nu_n^2 \right\} r \frac{\partial}{\partial r} + \left\{ 7 - 2\nu_n^2 \right\} r^2 \frac{\partial^2}{\partial r^2} + 6r^3 \frac{\partial^3}{\partial r^3} + r^4 \frac{\partial^4}{\partial r^4} \\ &\quad + \left\{ (\omega^2 - \mu_1^2) + 5(\omega^2 - \mu_2^2) \right\} r^3 \frac{\partial}{\partial r} + \left\{ 2\omega^2 - \mu_1^2 - \mu_2^2 \right\} r^4 \frac{\partial^2}{\partial r^2}. \end{aligned} \quad (3.22)$$

The large r behaviour of $\tilde{J}_n^{(\frac{1}{2}, \pm)}$ may be picked out. There are two possibilities for

each case:

$$\begin{aligned} J^{(1)} &\sim r^{-1/2} \exp irk_1 & \text{and} & & J^{(2)} &\sim r^{-1/2} \exp irk_2 \\ J^{(1)} &\sim r^{-5/2} \exp irk_2 & & & J^{(2)} &\sim r^{-5/2} \exp irk_1, \end{aligned} \quad (3.23)$$

where $k_1 = \sqrt{\omega^2 - \mu_1^2}$ and $k_2 = \sqrt{\omega^2 - \mu_2^2}$. This neatly represents the two different possible excitations at large r that the system possesses. These persist to small r but are modified by the interaction.

We can use equation (3.5) to specify the large r behaviour in terms of two unknown coefficients α and β :

$$\rho = \left(\begin{array}{c} \frac{-\beta i(\mu_1^2 - \mu_2^2)}{(n + \frac{1}{2})} \frac{1}{\sqrt{r}} e^{k_1 r} + \frac{-\alpha i(n + \frac{1}{2})}{(\mu_2^2 - \mu_1^2)} \frac{1}{r^{5/2}} \cos(k_2 r + \delta) \\ \frac{\alpha}{\sqrt{r}} \cos(k_2 r + \delta) + \frac{\beta}{r^{5/2}} e^{k_1 r} \end{array} \right) e^{i(n + \frac{1}{2})\phi}. \quad (3.24)$$

We note that neither are oscillatory for $\omega^2 \leq \mu_1^2$ and only the lower mass excitation is for the intermediate range $\mu_2^2 < \omega^2 < \mu_1^2$. The solutions may however be exponentially decaying or growing in the non-oscillatory regions, and this behaviour should be established to understand the spectrum of the theory.

Having boiled the problem down to determining β and δ in equation (3.24), the problem is to understand which of the possible asymptotic forms these solutions are tending to. The next section is devoted to a powerful method of determining the large r behaviour of a series solution to an homogeneous linear ordinary differential equation.

Constructing a Contour Integral. A more powerful method is obviously required and the method used for Bessel functions with some modifications is used, constructing a complex contour integral (a type of Laplace transform) that solves the wave equation.

Let us look for a complex contour integral that satisfies the differential equation $\nabla_n \Phi = 0$. If we choose Φ to be

$$\Phi(r) = r^{k_0} \int_a^b T(t) e^{irt} dt \quad (3.25)$$

then we find that T must satisfy

$$atT + (b + ct^2)T' + (dt + et^3)T'' + (f + gt^2 + ht^4)T''' = 0 \quad (3.26)$$

where the coefficients are

$$\begin{aligned} a &= (1 - 2k_0)(2k_0 - 1 - 2[k_0^2 - \nu_n^2]) \\ b &= (2\omega^2 - \mu_1^2 - \mu_2^2)(k_0^2 - \nu_n^2 - 2k_0 + 2) + (\mu_1^2 - \mu_2^2)(2k_0 - 2) \\ c &= 2\nu_n^2 - 6k_0^2 + 12k_0 - 7 \\ d &= (3 - 2k_0)(2\omega^2 - \mu_1^2 - \mu_2^2) - 2(\mu_1^2 - \mu_2^2) \\ e &= 4k_0 - 6 \\ f &= -(\omega^2 - \mu_1^2)(\omega^2 - \mu_2^2) \\ g &= 2\omega^2 - \mu_1^2 - \mu_2^2 \\ h &= -1, \end{aligned} \quad (3.27)$$

and the integral is restricted to ensure the integration by parts steps were valid to get the above formula. These terms are of the form

$$[t^m T'' e^{irt}]_a^b, \quad [t^m T' e^{irt}]_a^b, \quad [t^m T e^{irt}]_a^b, \quad (3.28)$$

for various powers m between 0 and 4, of t . Thus the path must either begin and end at $t = +i\infty$ (as $r > 0$ everywhere) or it must be a closed path. Re-writing the equation

$$atT + (b + ct^2)T' + (dt + et^3)T'' - (t^2 - \omega^2 + \mu_1^2)(t^2 - \omega^2 + \mu_2^2)T''' = 0, \quad (3.29)$$

the regular singular points at $t^2 = \omega^2 - \mu_1^2, \omega^2 - \mu_2^2$, are obvious. The small t behaviour is calculable: expand T as

$$T = \sum_{m=0}^{\infty} a_m t^m, \quad (3.30)$$

and the resulting recursion relation is

$$\begin{aligned}
& a_{m-1}\{a + c(m-1) + e(m-1)(m-2) + h(m-1)(m-2)(m-3)\} \\
& + a_{m+1}\{b(m+1) + dm(m+1) + g(m-1)(m)(m+1)\} \\
& + a_{m+3}f(m+3)(m+2)(m+1) = 0.
\end{aligned} \tag{3.31}$$

The three independent solutions are generated by series beginning at $m = 0, 1, 2$.

$$\begin{aligned}
T &= 1 - \frac{a}{24f}t^4 + \dots \\
T &= t - \frac{b}{6f}t^3 + \dots \\
T &= t^2 - \frac{(b+d)}{12f}t^4 + \dots
\end{aligned} \tag{3.32}$$

and the recursion relations generate the rest of the solutions. The value of T is assumed to be finite at the origin. The large t behaviour of T is $T = t^\mu + \dots$ where μ is one of the roots of

$$\mu^3 h + \mu^2(e - 3h) + \mu(c - e + 2h) + a = 0. \tag{3.33}$$

The three possibilities are

$$\mu^{(\pm)} = \begin{cases} 2k_0^{(\pm)} - 1; \\ 2k_0^{(\pm)} - 1 \mp \text{sign}[n + \frac{1}{2}]; \\ \pm \text{sign}[n + \frac{1}{2}] - 1. \end{cases} \tag{3.34}$$

The first root is expected*, and from this the other two can be calculated.

Turning now to the behaviour at the singular point, use the method of Frobenius to find a solution. Assuming that a power series expansion exists starting at some

* see below—discussion of equation (3.47).

finite, not necessarily integer, number ν ,

$$T(t) = (t - A)^\nu + a_1(t - A)^{\nu+1} + \dots \quad (3.35)$$

Write

$$T(t) = \sum_{n=\nu, \nu+1, \dots}^{\infty} a_n(t - A)^n,$$

and the differential equation as

$$atT + (b + ct^2)T' + (dt + et^3)T'' - (t^2 - A^2)(t^2 - B^2)T''' = 0, \quad (3.36)$$

we establish the recursion relation for the a_n 's as

$$\begin{aligned} & a_{n-1} \{a + c(n-1) + e(n-1)(n-2) - (n-1)(n-2)(n-3)\} \\ & a_n \{aA + 2Acn + 3eAn(n-1) - 4An(n-1)(n-2)\} \\ & a_{n+1} \{(b + cA^2)(n+1) + (d + 3eA^2)n(n+1) - (5A^2 - B^2)n(n+1)(n-1)\} \\ & a_{n+2} \{(d + eA^2)A(n+2)(n+1) - 2A(A^2 - B^2)n(n+2)(n+1)\} = 0. \end{aligned} \quad (3.37)$$

The descending series is terminated only if

$$\nu = \begin{cases} 0, 1, k_0 + \frac{3}{2} & \text{for } A = \pm\sqrt{\omega^2 - \mu_1^2}; \\ 0, 1, k_0 - \frac{1}{2} & \text{for } A = \pm\sqrt{\omega^2 - \mu_2^2}. \end{cases} \quad (3.38)$$

We find that near $t^2 = \pm\sqrt{\omega^2 - \mu_1^2}$, $\nu = k_0 + \frac{3}{2}$, and near $t^2 = \pm\sqrt{\omega^2 - \mu_2^2}$, $\nu = k_0 - \frac{1}{2}$. These are the only branch points for the function in the complex t plane. As ω is increased the branch points move down the imaginary axis and then out along the real axis as shown in fig. 1. The possible solutions will be contour integrals that loop these singular points. The large r behaviour may be deduced from the regions immediately next to the singularities. We note that a loop around one of the branch points will pick up a factor $\exp iAr$, and so the points located on the imaginary axis

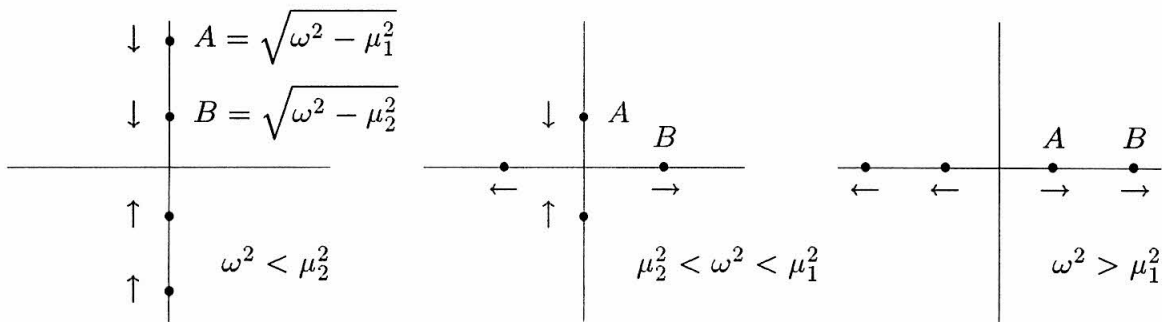


Fig. 1. Loci of the singular points of $T(t)$ in the complex t plane, as ω^2 increases.

will have exponential behaviour, and the points on the real axis will have oscillatory behaviour at large r . Integrate along the the contour shown in fig. 2 to find the large r asymptote: this is the standard contour considered for the large r asymptotic expansion of Bessel (Hankel) functions (*e.g.*, see Watson^[2]).

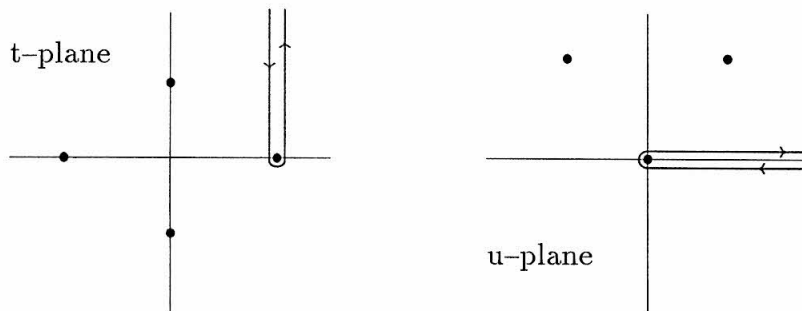


Fig. 2. Contours of integration, P_t and P_u in the t and u planes.

The leading power of r may be picked out by making the substitution $t - A = iu/r$, in the integrand. The same contour in the u plane is also shown in fig. 2. Writing $A = \sqrt{\omega^2 - \mu_1^2}$ and $B = \sqrt{\omega^2 - \mu_2^2}$ and evaluating the integral in the u -plane by expanding in powers of $1/r$, we find agreement with the large r evaluation above and extra information has shown up: namely the phase shifts and a prescription to obtain the higher corrections term by term. We can see a linear combination will pick out a sine (sinh) or cosine (cosh) function. The analogy to Bessel functions is now apparent.

$$\begin{aligned}
\Phi(r)_2 &= r^{k_0} \oint_{P_t} T(t) e^{irt} dt \\
&= r^{k_0 - k_0 + \frac{1}{2} - 1} e^{i(Br + \frac{\pi}{2}[k_0 - \frac{1}{2} + 1])} \oint_{P_u} u^{k_0 - \frac{1}{2}} (1 + a_1 \frac{u}{r} + \dots) e^{-u} du \\
\Phi(r)_2 &= r^{k_0} \oint_{P_t} T(t) e^{irt} dt \\
&= r^{k_0 - k_0 - \frac{3}{2} - 1} e^{i(Ar + \frac{\pi}{2}[k_0 + \frac{3}{2} + 1])} \oint_{P_u} u^{k_0 + \frac{3}{2}} (1 + a_1 \frac{u}{r} + \dots) e^{-u} du.
\end{aligned} \tag{3.39}$$

An important subtlety pertains to the phases. We have to compare the values of the large r expansion of the solutions and this is dependent on the relative phase of the function $T(t)$ at the branch points. For example, the case of Bessel functions is particularly straightforward as the function $T(t)$ which generates a ν th order Bessel function $J_\nu(kr)$, with the same form of contour integral

$$\Phi(r) = r^\nu \int_a^b T(t) e^{irt} dt \tag{3.40}$$

is simply

$$T(t) = (t^2 - k^2)^{\nu - \frac{1}{2}}. \tag{3.41}$$

There are two branch points for general ν and the two possibilities for paths (the

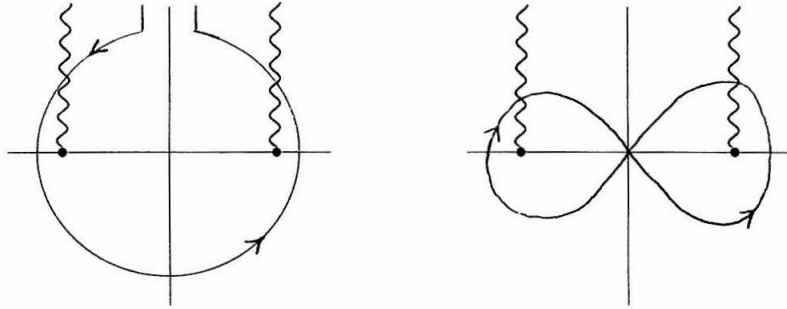


Fig. 3. The two contours that produce linearly independent solutions.

two linearly independent solutions) are shown in fig. 3. The figure eight around the branch points gives the solutions that are finite at the origin, and the other gives a linearly independent solution which blows up at the origin, $J_\nu(r)$ and $J_{-\nu}(r)$. Having already calculated the asymptotic expansion to the branch point at $t = +1$ (I called it $t = +B$ for a Bessel function of order k_0), the other branch point traversed in the opposite direction will give the large r expansion of J_ν .

$$\begin{aligned}\Phi(r)_2^{(-|B|)} &= r^{k_0} \oint_{P_t} T(t) e^{irt} dt \\ &= r^{k_0 - k_0 + \frac{1}{2} - 1} e^{i(-|B|r + \frac{\pi}{2}[k_0 - \frac{1}{2} + 1 + 2(k_0 - \frac{1}{2}) - 2])} \oint_{P_u} u^{k_0 - \frac{1}{2}} (1 + a_1 \frac{u}{r} + \dots) e^{-u} du\end{aligned}\quad (3.42)$$

The terms are the same except for adding into the phase the overall $(-1)^{k_0 - \frac{1}{2}}$ coming from the phase of the function $T(t)$ and an extra negative to traverse the path in the opposite direction (this negative permitted both paths to begin on the same sheet and hence exclude any phase factors associated with the sheet). Note that general ν is permitted as the branch cuts are first traversed one way, then the other, and hence the integral is unambiguous for any ν . Thus adding both these terms, the correct behaviour of Bessel functions is obtained,

$$J_{k_0}(|B|r) = \frac{e^{i\pi[k_0 + \frac{1}{2}]}}{\sqrt{r}} \cos(|B|r - \frac{\pi}{2}[k_0 + \frac{1}{2}]) (1 + O(1/r^2)), \quad (3.43)$$

with an overall phase factor which may be absorbed into the definition of $T(t)$.

It is clear, then, that the overall phase of the solution is needed and hence more information about $T(t)$ is needed.

Firstly, recall that we are only interested in the solution for ρ_2 , the second component, as the equations of motion may be used to evaluate the first component's behaviour at large r as in equation (3.24).

$$\begin{aligned}\Phi_2(r) &= r^{k_0} \oint_{P_B} dt e^{irt} T(t) \\ T(t) &= N(t^2 - A^2)^{k_0 + \frac{3}{2}} (t^2 - B^2)^{k_0 - \frac{1}{2}},\end{aligned}\quad (3.44)$$

The four branch points at $t = \pm|B|, \pm i|A|$, make a contribution to the large r behaviour. Assume first of all that all the branch points are present in *one* of the three possible solutions for $T(t)$. If we introduce cuts that lead off to imaginary infinity where the integral is damped, then the solution which starts at r^{-k_0} is generated by a contour wrapping all of the singular points and leading off to infinity as in fig. 4.

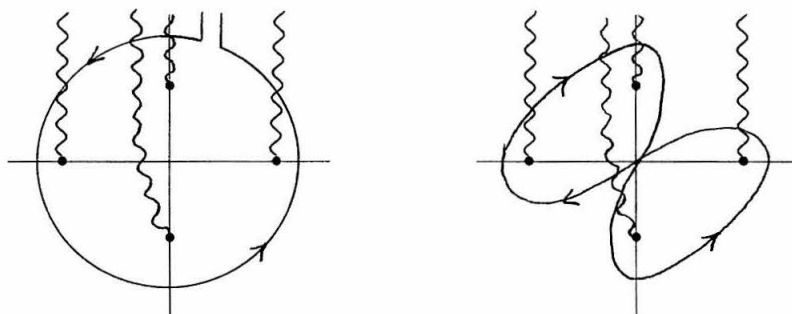


Fig. 4. Possible contours of integration, P_t , in the t -plane.

Expanding $T(t)$ in powers of t^{-1} which is uniformly convergent on the contour and letting the contour radius go off to infinity, the first nonzero coefficient of $\tilde{J}_{-k_0}(r)$, a_{-k_0} is seen to be

$$a_{-k_0} = \lim_{r \rightarrow 0} r^{k_0} \Phi_2(r) = (-i)^{2k_0} \left[\frac{d^{2k_0-1}}{dt^{2k_0-1}} T(t) \right]_a^b, \quad (3.45)$$

where a and b are the curve's end points. This term is nonzero if the total phase difference of circling the four branch points is non-zero (which, incidentally, is not the case for $4k_0 \in \mathbb{Z}$ but analytic continuation still allows this method to determine the large r behaviour). This was the reason that a solution that went to t^{2k_0-1} was expected as a root for the large r behaviour of the differential equation. However, it is crucial to note that there are two other possible large t behaviours for the function $T(t)$ listed in equation (3.34).

$$\mu^{(\pm)} = \begin{cases} 2k_0^{(\pm)} - 1; \\ 2k_0^{(\pm)} - 1 \mp \text{sign}[n + \frac{1}{2}]; \\ \pm \text{sign}[n + \frac{1}{2}] - 1. \end{cases} \quad (3.46)$$

By the same reasoning as above, the contour of fig. 4 enclosing all of the branch points corresponds to various lowest powers of r : for each case, $-k_0^{(\pm)}$, $-k_0^{(\mp)}$, $k_0^{(\mp)}$. The sense of this is apparent: the “other” possible solutions, besides the one beginning at the power $k_0^{(\pm)}$, are accessed, *i.e.*, similar to the Bessel function case where there is only one other solution. The solution beginning at $k_0^{(\pm)}$ is represented by a closed contour integral such as that in fig. 4. Appendix A points out the fact that the equation for $T(t)$ is in fact second order in the $a = 0$ ($k_0 = k_0^U$) regime. In the $a = 0$ regime the solution $T = 1$ is present and thus gives trivial answers for the closed contour integrals (*i.e.*, the method of a contour integral does not work). In the $\tilde{a} = 0$ ($k_0 = k_0^L$) regime the function representing $\tilde{J}_{-k_0^U}(r)$ is a finite polynomial in only positive powers of t —its closed contour integral is zero. Thus the solutions cannot represent this function.

If we had all three exact solutions, we could choose the one with large r behaviour t^{2k-1} as for Bessel functions, then the closed contour integrals would give uniquely the large r behaviour for the “ \pm ” modes and, in the intermediate energy range, they could be combined to cancel the exponential divergences and produce a finite large r behaviour going as

$$\alpha\rho_2^{(+)} + \beta\rho_2^{(-)} \sim \frac{1}{\sqrt{r}} \cos(k_2 r + \delta).$$

Even without the full solution the method still bears fruit.

Theorem. At least one solution exists with a branch point at $t^2 = B^2$ of power $k_0 - \frac{1}{2}$ and one with a branch point at $t^2 = A^2$ of power $k_0 + \frac{3}{2}$, for each k_0 .

The solutions must have the following generic behaviours

$$\begin{aligned} T_B &= Q_B(t)(t^2 - B^2)^{k_0 - \frac{1}{2}}, \\ T_A &= Q_A(t)(t^2 - A^2)^{k_0 + \frac{3}{2}}, \end{aligned} \tag{3.47}$$

where $Q_B(t)$ may or may not have a branch point in it at $t^2 = A^2$, but it is a nonzero constant at $t^2 = B^2$ and the equivalent is true for $Q_A(t)$. This is true by explicit

construction of such a solution starting at $t^2 = B^2$ and using the generating formulae of equations (3.37) and (3.38) and similarly for $t^2 = A^2$.

The large t behaviour of $T(t)$ is, generically, a mix of the three solutions

$$T \sim \alpha t^{\mu_1} + \beta t^{\mu_2} + \gamma t^{\mu_3},$$

where $\mu_1 = 2k_0^{(\pm)} - 1$, $\mu_2 = 2k_0^{(\pm)} - 1 \mp \text{sign}[n + \frac{1}{2}]$, and $\mu_3 = \pm \text{sign}[n + \frac{1}{2}] - 1$. The open contour enclosing these points gives the mixture

$$\Phi_2^{open}(r) = \alpha \tilde{J}_{-k_0^{(\pm)}}(r) + \beta \tilde{J}_{-k_0^{(\mp)}}(r) + \gamma \tilde{J}_{k_0^{(\mp)}}(r) \quad (3.48)$$

for some (unknown, complex and possibly zero) values of α , β and γ . The closed contour integral also gives, generically, a mixture of two solutions

$$\Phi_2^{closed}(r) = \alpha \tilde{J}_{k_0^{(\pm)}}(r) + \beta \tilde{J}_{k_0^{(\mp)}}(r). \quad (3.49)$$

The issue is now, which solutions are present? Consider closed contours first. The value of the coefficient of the *lowest* power of r for the closed contour integral

$$a_{k_0} = \oint T(t) dt, \quad (3.50)$$

is clear and the next coefficient will determine the amount of the other solution added in

$$a_{k_0+1} = i \oint tT(t) dt. \quad (3.51)$$

In the case of Bessel functions, this is seen to be zero by taking the closed contour integral of the first order differential equation for $T(t)$.

Letting this contour integral operate on the entire differential equation for $T(t)$ in this case shows

$$\begin{aligned}
& \oint dt \{ atT + (b + ct^2)T' + (dt + et^3)T'' - (t^2 - \omega^2 + \mu_1^2)(t^2 - \omega^2 + \mu_2^2)T''' \} \\
&= \oint dt tT(a - 2c + 6e + 24) \\
&= \begin{cases} 4k(2k + 1) \oint tT dt & \text{for } a = 0; \\ 0 & \text{for } \tilde{a} = 0, \end{cases} \tag{3.52}
\end{aligned}$$

where $\tilde{a} = a - 2c + 6e + 24$ (see equation (3.27) for the values of $a \dots e$). The condition $a = 0$ boils down to the cases where $k_0 = k_0^U$, where k_0^U is the higher of the two possible values for the k_0 , $|n|$ and $|n + 1|$. The other condition, namely $\tilde{a} = 0$ is $k_0 = k_0^L$, the lower of the two values.

$$k_0^L = \begin{cases} |n| & \text{for } n \geq 0; \\ |n + 1| & \text{for } n \leq -1. \end{cases} \tag{3.53}$$

For the case $k_0 = k_0^U$ we have ensured that all lower coefficients are zero and so there is no other solution present apart from $\tilde{J}_{-k_0^{(\pm)}}(r)$, *i.e.*, the other solution would have to start at the power of r that is an integer lower than k_0^U . This is entirely consistent with equation (3.53) because it shows that $a_{k_0+1} = 0$ in the $k_0 = k_0^U$ case only. For the other cases we do not know whether there is any of the other function added in, and we must assume that in general there is.

Next, consider open contours, which we mention merely for completeness as they are not required for the later argument. For $k_0 = k_0^U$ there is no $\tilde{J}_{k_0^{(\mp)}}(r)$ solution because the descending series, beginning at t^0 , that would generate this solution terminates, $T = 1$ trivially. Further, for $k_0 = k_0^L$ there is no $\tilde{J}_{-k_0^{(\mp)}}(r)$ solution, again, because the descending series terminates at a positive power of t . Thus the possible mix of functions is schematically shown in table 2.

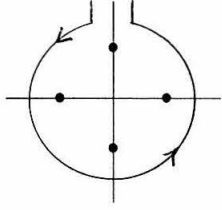
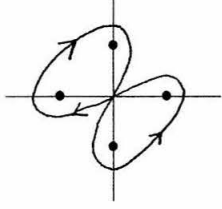
| Contour | $\Phi(r)$ for $k_0 = k_0^L$ | $\Phi(r)$ for $k_0 = k_0^U$ |
|---|---|---|
|  | $\sim \alpha \tilde{J}_{-k_0^L} + \gamma \tilde{J}_{k_0^U}$ | $\sim \alpha \tilde{J}_{-k_0^U} + \beta \tilde{J}_{-k_0^L}$ |
|  | $\sim \alpha' \tilde{J}_{k_0^L} + \beta' \tilde{J}_{k_0^U}$ | $\sim \tilde{J}_{k_0^U}$ |

Table 2. Possible functions represented by the possible contours.

Returning to study solely the relevant case of closed contours, let us deal with the case $\tilde{a} = 0$ first. The function Φ has possible contributions from the two functions $\tilde{J}_{k_0^U}(r)$ and $\tilde{J}_{k_0^L}(r)$ in unknown proportions. Another statement of this fact is that there are two possible non-trivial contours that are closed and well defined: figure eights around the branch points at $t = \pm|B|$ and $t = \pm i|A|$ for the intermediate energy range. Taking a linear combination gives the contour shown in fig. 4. Taking the standard deformation to obtain the large r expansion shown in fig. 5, we may evaluate the large r expansion taking $Q(A)/Q(B)$ as unknown.

Let the parts of the contour parallel to the real axis be sent away to imaginary infinity so, because of damping by the exponential, they will not contribute. Then the usual $t - A = iu/r$ substitution is made, and the terms of an expansion of T in $(t - A)$ gives the expansion in $1/r$. All of the phases are chosen to have a particular value at the point marked with an \times and the phases of the factor functions of $T(t)$ calculated from there following the path in its indicated direction of traversal. The phases are chosen to be zero along their respective cut lines, by adjusting the starting phase at \times .

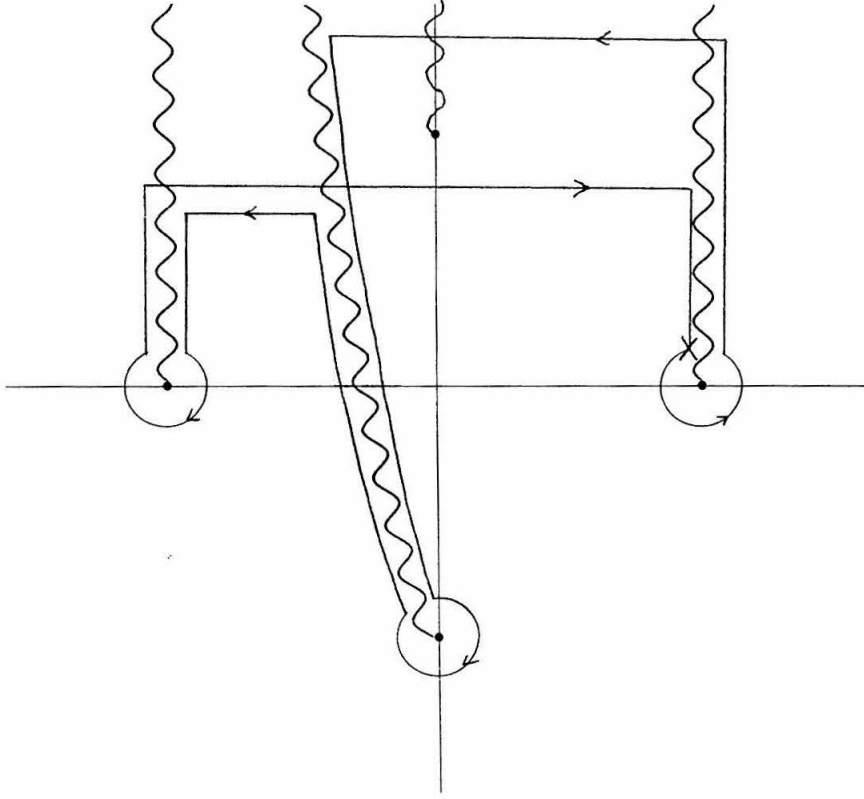


Fig. 5. Deformation of the contour that leads to an asymptotic large r expansion.

Firstly, the part of the contour looping around the branch point at $t = +|B|$ makes a contribution to the Φ_2 solution

$$\begin{aligned}\Phi_2^{+|B|} &\sim \frac{Q(|B|)}{\sqrt{r}} \exp(iBr + i\frac{\pi}{2}[(k_0 - \frac{1}{2} + 1) + 3(k_0 - \frac{1}{2}) + 2(k_0 + \frac{3}{2})]) \\ &= Q(|B|) \frac{e^{i\frac{\pi}{2}[7k_0 + \frac{5}{2}]}}{\sqrt{r}} \exp(iBr - i\frac{\pi}{2}[k_0 + \frac{1}{2}]).\end{aligned}\quad (3.54)$$

The term $(k_0 - \frac{1}{2} + 1)$, comes from the leading term in $T(t)dt$, $(t - B)^{k_0 - \frac{1}{2}} dt$, because the substitution $(t - B) = iu/r$ was made, see above—equation (3.39). The next part comes from the phase of the function $(t + B)^{k_0 - \frac{1}{2}}$ and the last part from the phase of the function $(t^2 - A^2)^{k_0 + \frac{3}{2}}$. The branch point at $t = -|B|$ contributes

the following

$$\begin{aligned}\Phi_2^{-|B|} &\sim \frac{Q(-|B|)}{\sqrt{r}} \exp(-i|B|r + i\frac{\pi}{2}[k_0 - \frac{1}{2} + 1 - 2 + 5(k_0 - \frac{1}{2}) + 2(k_0 + \frac{3}{2})]) \\ &= Q(-|B|) \frac{e^{i\frac{\pi}{2}[7k_0 + \frac{5}{2}]}}{\sqrt{r}} \exp(-i|B|r + i\frac{\pi}{2}[k_0 + \frac{1}{2}]).\end{aligned}\tag{3.55}$$

The loop around $t = +i|A|$ gives a large r behaviour that is suppressed as $\exp -|A|r$ and so may be neglected. The contribution from the loop around the branch point at $t = -i|A|$ is

$$\begin{aligned}\Phi_2^{-i|A|} &\sim Q(-i|A|) \frac{4sF^{k_0 - \frac{1}{2}}}{r^{\frac{5}{2}}|A|^2} \exp(|A|r + i\frac{\pi}{2}[k_0 + \frac{3}{2} + 1 - 2 + 8(k_0 - \frac{1}{2}) + 2(k_0 + \frac{3}{2})]) \\ &= \frac{4Q(-i|A|)}{r^{\frac{5}{2}}|A|^2} F^{k_0 - \frac{1}{2}} s \exp(-|A|r) e^{-3i\pi/2},\end{aligned}\tag{3.56}$$

where

$$\begin{aligned}s(\omega) &= \left| \frac{\mu_1^2 - \omega^2}{\mu_2^2 - \mu_1^2} \right|^2, \\ F(\omega) &= \left| \frac{\omega^2 - \mu_1^2}{\omega^2 - \mu_2^2} \right|^{\frac{1}{2}}.\end{aligned}\tag{3.57}$$

Single figure eight contour integrals around the $t = \pm|B|$ give the same result for their behaviour. To finish the calculation, the value $Q(t)/Q(-t)$ is needed. The following ansatz is discussed below, but is later replaced by a precise value obtained by matching to the $\Gamma \rightarrow 0$ limit (*i.e.*, no mass splitting or interaction).

Ansatz: $Q(t)$ is even: $Q(t) = Q(-t)$.

We know from the even operator that the solutions have definite parity and we have found trivial even solutions in Appendix 3A, thus $Q(t)$ is either odd or even. The actual solutions with the leading behaviour $(t^2 - A^2)^{k_0 + 3/2} (t^2 - B^2)^{k_0 - 1/2}$ may be a mix of both, and indeed we find this to be the case. For clarity we continue with the even case only.

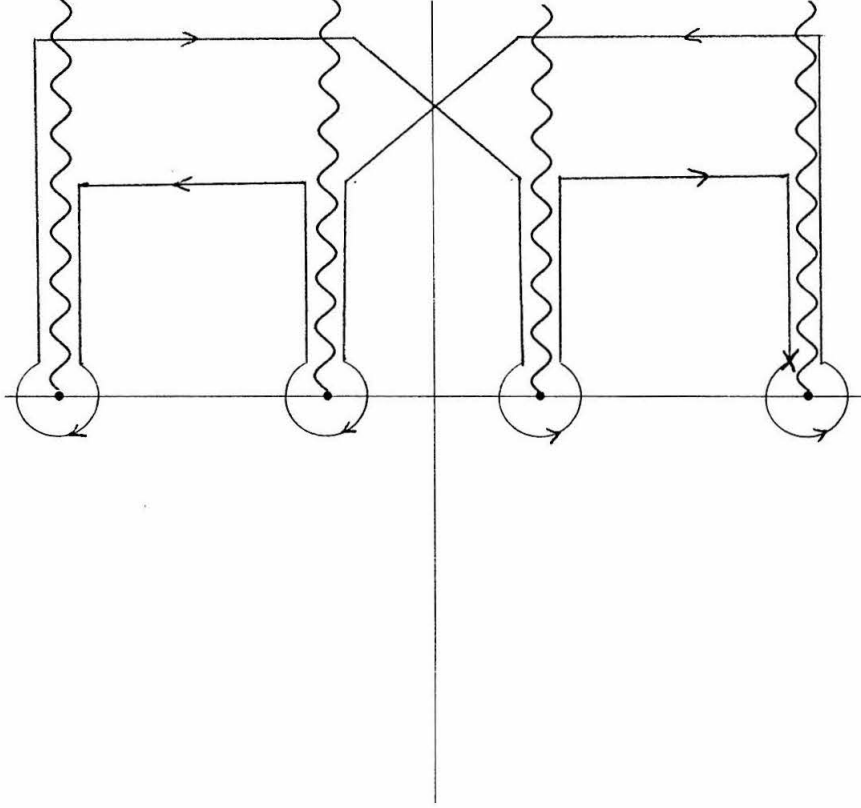


Fig. 6. Deformation of the contour in the high energy regime.

Proceeding, we can see that the (uncalculated) combination of solutions of order $k_0^{(+)}$ and $k_0^{(-)}$ that has cancelled the exponential behaviour at large r is

$$\rho_2^n = \alpha \tilde{J}_{k_0^{(+)}}(r) + \beta \tilde{J}_{k_0^{(-)}}(r) \sim \frac{1}{\sqrt{r}} \cos(k_2 r - \frac{\pi}{2}[k_0^L + \frac{1}{2}]), \quad (3.58)$$

where $a = 0$ ensures the value k_0 is unique: the lower of $|n|$ and $|n + 1|$.

The $a = 0$ condition ensures that the solution is unique for each n as it is equivalent to $k_0 = k_0^L$: the lower of $|n|$ and $|n + 1|$.

The other case $\tilde{a} = 0$ must, then, be superfluous. It is inconsistent to attempt to construct solutions from the $\tilde{a} = 0$ regime; they must not be present. Their existence would lead to a logical inconsistency: the closed contour corresponds to a

unique solution that begins at a certain power of r but has no reference to one of the momenta in its large r expansion.

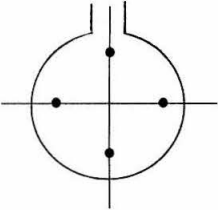
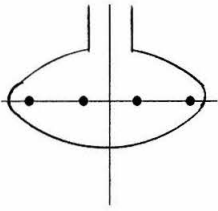
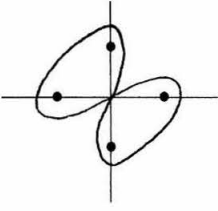
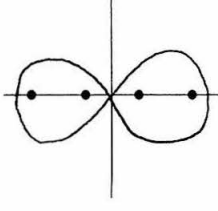
| Contour | Behaviour of the integral $\Phi(r)$ |
|---|---|
|  | $\frac{1}{\sqrt{r}} \sin \left(k_2 r - \frac{\pi}{2} [k_0^L + \frac{1}{2}] \right) - \frac{(-)^{k_0^L} x}{2r^{5/2}} e^{k_1 r}$ |
|  | $\frac{1}{\sqrt{r}} \sin \left(k_2 r - \frac{\pi}{2} [k_0^L + \frac{1}{2}] \right) + \frac{x}{r^{5/2}} \sin \left(k_1 r - \frac{\pi}{2} [k_0^L + \frac{1}{2}] \right)$ |
|  | $\frac{1}{\sqrt{r}} \cos \left(k_2 r - \frac{\pi}{2} [k_0^L + \frac{1}{2}] \right) - \frac{i(-)^{k_0^L} x}{2r^{5/2}} e^{k_1 r}$ |
|  | $\frac{1}{\sqrt{r}} \cos \left(k_2 r - \frac{\pi}{2} [k_0^L + \frac{1}{2}] \right) - \frac{ix}{r^{5/2}} \cos \left(k_1 r - \frac{\pi}{2} [k_0^L + \frac{1}{2}] \right)$ |

Table 3. Possible large r behaviours.

This cannot be the case as a single solution must behave as a mix of Bessel functions for both particles. But as there must exist solutions with branch points in, we are in danger of a contradiction. The only self consistent way out is that the solution

is odd for $k_0 = k_0^U$. The substitution $t \rightarrow -t$ in the expression for a_{k_0} of equation (3.50) demonstrates that it is identically zero.

The case of large energy is similarly calculable. The contour shown in fig. 4 is deformed as the branch points move out along the real axis and the large r asymptote is then calculated by the integral round the contour shown in fig. 6. An analogous calculation to that presented above results in

$$\Phi_2 \sim \frac{Q(B)}{\sqrt{r}} \cos(k_2 r - \frac{\pi}{2}[k_0 + \frac{1}{2}]) - i \frac{(-)^{k_4} 4 F^{k_0 - \frac{1}{2}} s}{r^{5/2} |A|^2} Q(A) \cos(k_1 r - \frac{\pi}{2}[k_0 + \frac{1}{2}]). \quad (3.59)$$

All of the possible large r behaviours are contained in the four calculations of contour integrals of $T(t)$ shown schematically in table 3. In table 3

$$x = (-)^{k_0^L} \frac{4 F^{k_0^L - \frac{1}{2}} s}{|A|^2} \frac{Q(A)}{Q(B)}. \quad (3.60)$$

All of the contours may be broken down into their respective two parts containing pairs of the singularities, *e.g.*, the figure eights can wrap the points at $t = \pm|A|$ only or at $t = \pm|A|$ only. The same large r behaviours are obtained. Thus the large r behaviours are all known.

Determining the value of $Q(A)/Q(B)$. To check that we are doing the calculation correctly, we may solve the system completely for the mass splitting zero case and the large r behaviours should match. This check turns out to give us the value for $Q(A)/Q(B)$, and so the problem is solved completely.

Equations (3.5) and (3.6) may be solved in the case that $\mu_1^2 = \mu_2^2 = m^2$, for an energy $\omega^2 > m^2$,

$$\begin{aligned} (\omega^2 - L)\rho_1 &= -\frac{1}{r^2} \partial_\phi \rho_2 \\ (\omega^2 - L)\rho_2 &= \frac{1}{r^2} \partial_\phi \rho_1, \end{aligned} \quad (3.61)$$

where $L = -\nabla^2 + \frac{1}{4r^2} + m^2$ and ρ_2 satisfies

$$r^2(\omega^2 - L)r^2(\omega^2 - L)\rho_2 = -\partial_\phi^2 \rho_2. \quad (3.62)$$

Either of the following two vectors solve the problem:

$$\rho_{\Gamma=0}^{(+)} = \begin{pmatrix} J_{k_0^{(+)}} \\ iJ_{k_0^{(+)}} \end{pmatrix} e^{i(n+\frac{1}{2})\phi} e^{-i\omega t} \quad \rho_{\Gamma=0}^{(-)} = \begin{pmatrix} J_{k_0^{(-)}} \\ -iJ_{k_0^{(-)}} \end{pmatrix} e^{i(n+\frac{1}{2})\phi} e^{-i\omega t}, \quad (3.63)$$

where J_ν (no tilde) is the usual Bessel function of order ν . Why are there two solutions? Take the real and imaginary parts of these complex solutions to get the values ρ_1 and ρ_2 and hence find η to be,

$$\eta^{(\pm)} = \begin{cases} J_{k_0^{(+)}} e^{-i(n+1)\phi} e^{i\omega t}, \\ J_{k_0^{(-)}} e^{in\phi} e^{-i\omega t}. \end{cases} \quad (3.64)$$

Comparing equations (3.18) and (3.63), it is apparent that regular Bessel functions are the limit of the modified Bessel functions as the mass splitting goes to zero,

$$\tilde{J}_{k_0}^{(1,2)} \rightarrow J_{k_0}. \quad (3.65)$$

We know the large r behaviour of both the upper and lower components from equation (3.24),

$$\rho = \begin{pmatrix} \frac{-\beta i(\mu_1^2 - \mu_2^2)}{(n+\frac{1}{2})} \frac{1}{\sqrt{r}} e^{k_1 r} + \frac{-\alpha i(n+\frac{1}{2})}{(\mu_2^2 - \mu_1^2)} \frac{1}{r^{5/2}} \cos(k_2 r + \phi) \\ \frac{\alpha}{\sqrt{r}} \cos(k_2 r + \phi) + \frac{\beta}{r^{5/2}} e^{k_1 r} \end{pmatrix}, \quad (3.66)$$

and so this matching will give a value for $Q(A)/Q(B)$. It ensures that as the mass splitting goes to zero, there is absolutely no scattering; a free field theory of η is left as $\Gamma \rightarrow 0$.

Working in the upper energy regime, the solution is found by requiring $\Phi(r)$ to have a real and imaginary part that are the lower (real) components of the functions

$$\rho^U = \frac{i}{\sqrt{2}} \gamma (\rho_{\Gamma=0}^{(+)} + \rho_{\Gamma=0}^{(-)}), \quad \rho^L = \frac{-i}{\sqrt{2}} (\rho_{\Gamma=0}^{(+)} - \rho_{\Gamma=0}^{(-)}), \quad (3.67)$$

respectively, where $\gamma = \text{sign}[n + \frac{1}{2}]$. This fixes Φ as

$$\Phi \sim \frac{e^{i\pi/4}}{\sqrt{r}} \exp i \left(k_2 r - \frac{\pi}{2} [k_0^L + \frac{1}{2}] \right) - \frac{e^{i\pi/4} |n + \frac{1}{2}| k_2^{1/2}}{k_1^{1/2} (\mu_1^2 - \mu_2^2) r^{5/2}} \exp -i \left(k_1 r - \frac{\pi}{2} [k_0^L + \frac{1}{2}] \right), \quad (3.68)$$

where $k_1 = |A|$ and $k_2 = |B|$. Then the value of the function $Q(t)$ can be read off

by comparing to Φ , calculated along the figure eight curve in the bottom diagram of table 3, multiplied by $e^{i\pi/4}$,

$$\begin{aligned}
Q(B) &= 1; \\
Q(-B) &= 0; \\
Q(A) &= 0; \\
Q(-A) &= \frac{-i}{4A^2} |n + \frac{1}{2}| \left| \frac{B}{A} \right|^{k_0^L}.
\end{aligned} \tag{3.69}$$

It is evident that $Q(t)$'s even and odd parts,

$$Q(t) = Q_{even}(t) + Q_{odd}(t), \tag{3.70}$$

satisfy $Q_{even}(B) = Q_{odd}(B)$ and similarly at $t = -A$.

The large r behaviour of Φ is valid for all mass splittings, but we are also interested in the intermediate energy regime. To calculate the behaviour in the intermediate energy range, we have to assume the form of $Q(t)$ as the same as in equation (3.69) with a phase factor $\exp(i\pi p/4)$. We cannot assume the function is analytic in A and B because these values appear in the coefficients of the differential equation (they are not variables) and so show up in $Q(t)$ also. The phase change will probably be such that p is an integer. The exact value of p is irrelevant to the generic form of the final result.

Thus, the real and imaginary parts of

$$\Phi = \frac{e^{i\pi/4}}{\sqrt{k_2 r}} \exp i \left(k_2 r - \frac{\pi}{2} [k_0^L + \frac{1}{2}] \right) - \frac{e^{i\pi/4[p+1]} (-)^{k_0^L} |n + \frac{1}{2}|}{k_1^{1/2} (\mu_1^2 - \mu_2^2) r^{5/2}} e^{k_1 r}, \tag{3.71}$$

give the large r behaviour of the functions in the intermediate energy regime. The real and imaginary parts are an unknown (orthogonal) combination of the two finite

solutions $\tilde{J}_{k_0^{(+)}}^{(2)}$ and $\tilde{J}_{k_0^{(-)}}^{(2)}$ which we parameterize by $\alpha(\Gamma, \omega^2, m^2)$,

$$\Phi = \exp i \left(\frac{\pi\gamma}{4} + \alpha \right) \left(\gamma \tilde{J}_{k_0^{(-)}}^{(2)} + i \tilde{J}_{k_0^{(+)}}^{(2)} \right). \quad (3.72)$$

Thus the large r expansions of the solutions are

$$\begin{aligned} \tilde{J}_{k_0^{(+)}}^{(2)} &\sim \begin{cases} \frac{1}{\sqrt{k_2 r}} \cos \left(k_2 r - \frac{\pi}{2} [k_0^{(+)} + \frac{1}{2}] - \alpha \right) + \frac{c}{\sqrt{k_1 r^{5/2}}} \cos \left(k_1 r - \frac{\pi}{2} [k_0^{(+)} + \frac{1}{2}] + \alpha \right); \\ \frac{1}{\sqrt{k_2 r}} \cos \left(k_2 r - \frac{\pi}{2} [k_0^{(+)} + \frac{1}{2}] - \alpha \right) - \frac{c\gamma(-)^{k_0^L}}{\sqrt{k_1 r^{5/2}}} e^{k_1 r} \sin \left(\frac{\pi}{4} [p + 1 - \gamma] - \alpha \right), \end{cases} \\ \tilde{J}_{k_0^{(-)}}^{(2)} &\sim \begin{cases} \frac{1}{\sqrt{k_2 r}} \cos \left(k_2 r - \frac{\pi}{2} [k_0^{(-)} + \frac{1}{2}] - \alpha \right) - \frac{c}{\sqrt{k_1 r^{5/2}}} \cos \left(k_1 r - \frac{\pi}{2} [k_0^{(-)} + \frac{1}{2}] + \alpha \right); \\ \frac{1}{\sqrt{k_2 r}} \cos \left(k_2 r - \frac{\pi}{2} [k_0^{(-)} + \frac{1}{2}] - \alpha \right) - \frac{c\gamma(-)^{k_0^L}}{\sqrt{k_1 r^{5/2}}} e^{k_1 r} \cos \left(\frac{\pi p}{4} - \alpha \right) \end{cases} \end{aligned} \quad (3.73)$$

where $c = (n + 1/2)/(\mu_1^2 - \mu_2^2)$ and it is clear that $\alpha(0, \omega^2, m^2) = 0$.

The finite part may now be read off: a linear combination of the $+$ and $-$ modes in the intermediate energy range and both of the modified Bessel functions in the upper range. We note that the large r behaviour of an orthogonal sum of the modified Bessel functions can be chosen to exactly match that of Bessel functions.

The modified Bessel functions look like Bessel functions at large r and it is only the next to leading order terms that will distinguish them,

$$\frac{1}{k_1 r} - \frac{1}{k_2 r} > 1 \quad (3.74)$$

and so they are similar for

$$r > R_0 = \frac{\sqrt{\Gamma}}{k_2^2} \quad (3.75)$$

for a typical wave length k_2 .

Classification of Solutions. The resulting behaviour at large r is now specified using

equation (3.24).

$$\begin{aligned}\rho_2 &= \frac{\alpha}{\sqrt{r}} \cos(k_2 r + \delta) + \frac{\beta}{r^{5/2}} e^{k_1 r} + \dots \\ \rho_1 &= \frac{-\beta i(\mu_1^2 - \mu_2^2)}{(n + \frac{1}{2})} \frac{1}{\sqrt{r}} e^{k_1 r} + \frac{-\alpha i(n + \frac{1}{2})}{(\mu_2^2 - \mu_1^2)} \frac{1}{r^{5/2}} \cos(k_2 r + \delta) + \dots\end{aligned}\tag{3.76}$$

The large r behaviour needs to fall off as fast as or faster than $1/\sqrt{r}$ in the first component and the normalisable combination found in the last section is

$$\rho_{low E} \sim \frac{1}{\sqrt{r}} \begin{pmatrix} O(1/r^2) \\ \cos(k_2 r - \delta_n) \end{pmatrix}\tag{3.77}$$

where $\delta_n = \frac{\pi}{2}[k_0^L + 1]$ for $k_0^L = \text{lower of } |n| \text{ and } |n + 1|$.

The resulting spectrum is shown schematically in table 4 classified by the large r behaviour of the solutions for each angular momentum eigenfunction. In table 4 $\delta_n = \frac{\pi}{2}[k_0^L + 1]$. This is the main result of this section. The evaluation of the phase shifts is all that is required to evaluate the cross section precisely.

| ω | $< \mu_2^2$ | $\mu_2^2 < \omega^2 < \mu_1^2$ | $\omega^2 > \mu_1^2$ |
|--------------|-------------|--|---|
| $\rho^{(+)}$ | 0 | 0 | $\begin{pmatrix} \frac{1}{\sqrt{2\pi k_1 r}} \cos\left(k_1 r - \frac{\pi}{2}[k_0^{(+)} + \frac{1}{2}]\right) \\ \frac{i}{\sqrt{2\pi k_2 r}} \cos\left(k_2 r - \frac{\pi}{2}[k_0^{(+)} + \frac{1}{2}]\right) \end{pmatrix}$ |
| $\rho^{(-)}$ | 0 | $\begin{pmatrix} O(1/r^{5/2}) \\ \frac{1}{\sqrt{2\pi k_2 r}} \cos(k_2 r - \delta_n) \end{pmatrix}$ | $\begin{pmatrix} \frac{1}{\sqrt{2\pi k_1 r}} \cos\left(k_1 r - \frac{\pi}{2}[k_0^{(-)} + \frac{1}{2}]\right) \\ \frac{-i}{\sqrt{2\pi k_2 r}} \cos\left(k_2 r - \frac{\pi}{2}[k_0^{(-)} + \frac{1}{2}]\right) \end{pmatrix}$ |

Table 4. The spectrum of the theory, large r behaviour.

3.3 CALCULATING THE CROSS SECTION.

The results we have obtained may now be applied to find the cross section of the theory. We shall first obtain the cross section in the intermediate energy range: $\mu_2^2 < \omega^2 < \mu_1^2$. The large r expansion of the single propagating mode (just the lower component) is

$$\rho_2^n = \sqrt{\frac{2}{\pi k_2 r}} \frac{1}{2} \left[e^{ik_2 r} e^{-i\delta_n} + e^{-ik_2 r} e^{i\delta_n} \right] e^{i(n+\frac{1}{2})\phi}, \quad (3.78)$$

where $\delta_n = \frac{\pi}{2}[k_0^L + 1]$. For convenience we re-write this

$$\rho_2^n = \sqrt{\frac{2}{\pi k_2 r}} \frac{1}{2} \left[e^{ik_2 r} e^{i\beta_{out}} + e^{-ik_2 r} e^{i\beta_{in}} \right] e^{i(n+\frac{1}{2})\phi}. \quad (3.79)$$

Now match a sum of these modes' ingoing parts $\exp(-ik_2 r)$, added up with a weight phase $\exp(i\alpha_n)$, to the incoming parts of a plane wave $e^{-ik_2 x}$, travelling down the x -axis from positive infinity,

$$\psi(t=0) = \sum_{n \in Z} \rho_2^n e^{i\alpha_n} = e^{i\phi/2} e^{-ik_2 r \cos \phi} + O\left(\frac{1}{\sqrt{r}}\right), \quad (3.80)$$

which may be expanded in terms of integer order Bessel functions as

$$e^{i\phi/2} e^{-ik_2 r \cos \phi} = \sum_{n \in Z} e^{-i\pi|n|/2} e^{i(n+\frac{1}{2})\phi} J_{|n|}(k_2 r). \quad (3.81)$$

The incoming parts match up at large distances if

$$\sqrt{\frac{2}{\pi k_2 r}} \frac{1}{2} \exp -i\left(k_2 r - \frac{\pi}{2}\left[|n| + \frac{1}{2}\right] + \frac{\pi|n|}{2}\right) = e^{i\alpha_n} \sqrt{\frac{2}{\pi k_2 r}} \frac{1}{2} \exp -i(k_2 r - \beta_{in}), \quad (3.82)$$

which defines α_n as $\alpha_n = \pi/4 - \beta_{in}$. The leading contribution to the outgoing part

of the solution ψ , may be read off,

$$\psi(t) = e^{i\phi/2} \left[e^{-ik_2x} + \frac{f(\phi)}{\sqrt{r}} e^{ik_2r} + O\left(\frac{1}{r}\right) \right] e^{-i\omega t} \quad (3.83)$$

where the scattering amplitude is

$$f(\phi) = \frac{1}{\sqrt{2\pi k_2}} \sum_{n \in \mathbb{Z}} e^{in\phi} e^{i(\frac{\pi}{4} + \beta_{out} - \beta_{in})}. \quad (3.84)$$

Reading the values of the phases from above, the result for the scattering amplitude is

$$f(\phi) = \frac{e^{-i\phi/2}}{\cos(\phi/2)} \frac{e^{i\pi/4}}{\sqrt{2\pi k_2}}. \quad (3.85)$$

This is exactly the Aharonov-Bohm scattering cross section for the entire intermediate energy range. Note however that the global charge eigenstate field from equation (3.2) is

$$\eta = \frac{1}{\sqrt{2}} (\rho_1 + i\rho_2) e^{-i\phi/2}, \quad (3.86)$$

where the fields ρ_1 and ρ_2 must be real. The linear real field equation that we have solved means that the real or imaginary part of any complex solution is also a solution. The scattering does not ‘look’ like the familiar Aharonov-Bohm form,

$$\eta = \frac{i}{\sqrt{2}} e^{-i\phi/2} \left(\cos(\phi/2 - k_2x - \omega t) + \frac{1}{\sqrt{r}} \frac{\cos(k_2r + \pi/4 - \omega t)}{\sqrt{2\pi k_2} \cos(\phi/2)} + O\left(\frac{1}{r}\right) \right). \quad (3.87)$$

but that depends on the observer’s viewpoint. Further note that to see this Aharonov-Bohm cross section, the observer will have to be further away than $R_0 = \frac{\sqrt{\Gamma}}{k_2^2}$ for incident momenta k_2 .

The high energy regime is similarly calculable. However, simply note that for a laboratory experiment bigger than $R_0 = \frac{\sqrt{\Gamma}}{k_2^2}$, the modes look exactly like Bessel functions and so an incoming plane wave, $\eta = e^{-ik_2x}$, will not be disturbed (*i.e.*, consider different boundary conditions than the low energy scattering case), if we only examine the system at distances greater than the boundary of influence that the vortex has.

The result, then, is that for scattering at energies between the two masses, we get exactly Aharonov-Bohm scattering, and for scattering at energies above the higher mass, we get perfect transmission. As the mass splitting goes to zero, the boundary of influence is reduced to zero, and the energy range, over which pure Aharonov-Bohm scattering occurs, is reduced to zero, leaving just pure unscattered plane waves in η , as the zero mass splitting limit of scattering off the vortex.

A slight ambiguity is that this sounds as if the cross section is discontinuous. This is not the case: it is a question of the order of limits. The lower modes can have the Aharonov-Bohm cross section at all energies if we just scatter pure ρ_2 modes. This is done by only exciting the k_0^L modes and not the k_0^U ones. In the lower energy regime, this gives the incoming wave and a scattered outgoing wave of Aharonov-Bohm cross section, but in the upper, the asymptotic forms include propagating upper components. Obtaining the same cross section in the lower modes gives a solution of the form:

$$\sum_{n \in Z} e^{i\alpha_n} \rho_n^L = \begin{pmatrix} ie^{i(\phi/2 - k_1 x)} [\delta(\phi + \pi)] + i \frac{e^{i\pi/4} e^{-ik_1 r}}{\sqrt{2\pi k_1 r} \sin(\phi/2)} \\ e^{i(\phi/2 - k_2 x)} [\delta(\phi)] + \frac{e^{-i\pi/4} e^{ik_2 r}}{\sqrt{2\pi k_2 r} \cos(\phi/2)} \end{pmatrix} + \dots \quad (3.88)$$

where the upper plane wave is propagating away down the negative x -axis and the lower is propagating toward the origin along the positive x -axis (the deltas are merely schematic to show the direction in which the asymptotic forms are valid). The two modes are clearly conjugate: the lower has a plane wave propagating into the vortex along the positive x -axis and scattered radially outward, and the upper has a mode propagating radially inwards and a plane wave scattered outward along the negative x -axis. Outside the radius that the vortex influences $R_0 = \sqrt{\Gamma}/k^2$, the asymptotic form is just that of Bessel functions (a particular orthogonal sum of the series starting at k_0^L and k_0^U will have to be made to achieve this, but it is possible) as in equation (3.63). The 1-D solution is clearly a sum of $\rho^{(-)}$ modes,

$$\rho = \begin{pmatrix} e^{-ik_1 x} \\ -ie^{-ik_2 x} \end{pmatrix} e^{i\phi/2} e^{-i\omega t} + O\left(\frac{1}{\sqrt{r}}\right), \quad (3.89)$$

and taking the real part of this solution the field η is

$$\eta = e^{-i\phi/2}(\cos(-k_1x + \phi/2 - \omega t) + i \sin(-k_2x + \phi/2 - \omega t)) + \dots, \quad (3.90)$$

which clearly has the correct limiting form: a pure unscattered wave as $\Gamma \rightarrow 0$, $\eta = \exp -i(kx + \omega t)$. A sum of $\rho^{(+)}$ modes gives a negative energy solution doing the same thing,

$$\rho = \begin{pmatrix} e^{-ik_1x} \\ ie^{-ik_2x} \end{pmatrix} e^{-i\phi/2} e^{-i\omega t} + \dots, \quad (3.91)$$

and $\eta \rightarrow \exp i(kx + \omega t)$. A sum of these two solutions shows that an incoming ρ_2 mode is scattered out as a ρ_1 mode, the asymptotic form is

$$\rho = \begin{pmatrix} e^{-ik_1x} \cos(\phi/2) \\ e^{-ik_2x} \sin(\phi/2) \end{pmatrix} e^{-i\omega t}. \quad (3.92)$$

3.4 NUMERICAL ANALYSIS.

To check the validity of this non-rigorous argument it is illuminating to perform a numerical analysis of the phase shifts for the low angular momentum eigenstates. This was done using Mathematica 2.1.

March-Russell *et al.* calculate the asymptotic phase shifts in the large angular momentum (n) limit to be pure Aharonov-Bohm, so the difference between the two calculations is most easily visible in the lowest angular momentum states.

The method used is to evaluate the series solution in increasing powers of r using equation (3.14). For chosen momenta k_1 and k_2 , and a particular angular momentum eigenvalue n , there are two series: one begins at $r^{|n|}$ and one at $r^{|n+1|}$. Each series is added up for the first coefficient value $b_{k_0} = 1$, and convergence for such an exponential series is good out to a some quite definite value of r . Choosing values in the energy range between the two masses the asymptotic form of a sum of an exponentially increasing curve and an oscillating component are apparent. The two

possible solutions are then evaluated over one wavelength of the oscillating component and the area under the curve multiplied by \sqrt{r} is adjusted to be zero by varying the ratio of the two series. If high enough powers of r have been evaluated this will give a converging value for the phase shift as the value of r , r_{test} say, at which the area is set to zero is increased. The main difficulty is that a difference of two exponentially divergent series is being taken and so a large number of significant figures may be required.

The value of k_2^2 was chosen to be 1000 so that by $r = 1$ about five wavelengths have occurred for low angular momentum states. Then k_1^2 was chosen to have various values so that the “small” parameter of March-Russell *et al.*; k_2^4/Γ^2 , takes values over four orders of magnitude. The convergence for increasing values of r_{test} is established by evaluating for various values. The imperfection of the test, *i.e.*, adding up the area to be zero, should show up as an oscillation of the same wavelength as the lower mass.

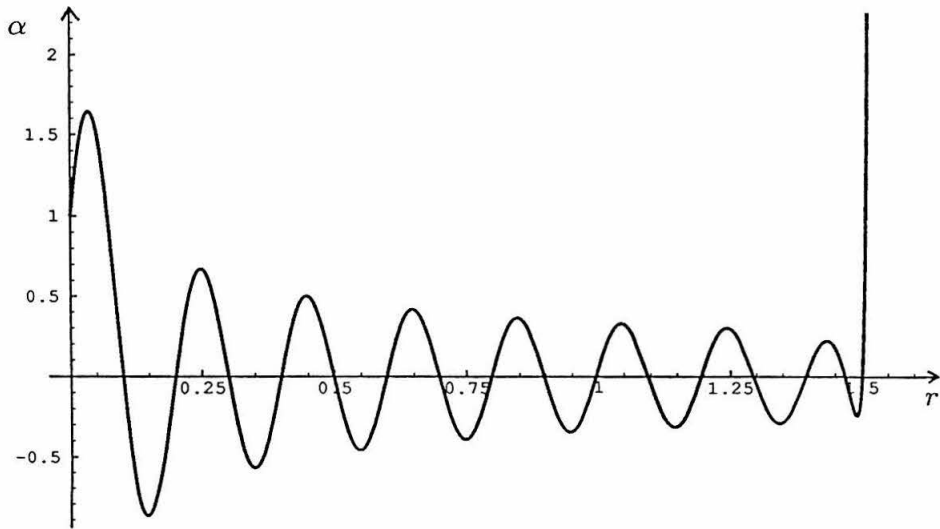


Fig. 7. Finite sum (at large r) of the two series for $n = 0$.

The sum of the two series is shown in fig. 7 for $n = 0$, $k_2^2 = -2000$ with a maximum power of r , $max = 162$, (*i.e.*, 81 terms in the series), working to 35 significant figures and evaluating the area by summing at twenty points ($m = 20$), over one wavelength

between $r = 1.45 - (2\pi)/k_2$ and $r = 1.45$ (*i.e.*, $r_{test} = 1.45$), the value of the function multiplied by \sqrt{r} . The difference of the phase shift to the pure Aharonov-Bohm phase shift $\alpha\pi$, is then calculated. The asymptotic form is

$$\tilde{J} \sim \frac{1}{\sqrt{r}} \cos(k_2 r - \frac{\pi}{2}[k_0^L + 1] - \alpha\pi) \quad (3.93)$$

and the value $\alpha = 0$ is predicted here whilst March-Russell *et al.* predict

$$\alpha = n + \frac{1}{2} - \left(\left(n + \frac{1}{2} \right)^2 + \frac{1}{4} \right)^{\frac{1}{2}}, \quad (3.94)$$

for positive n .

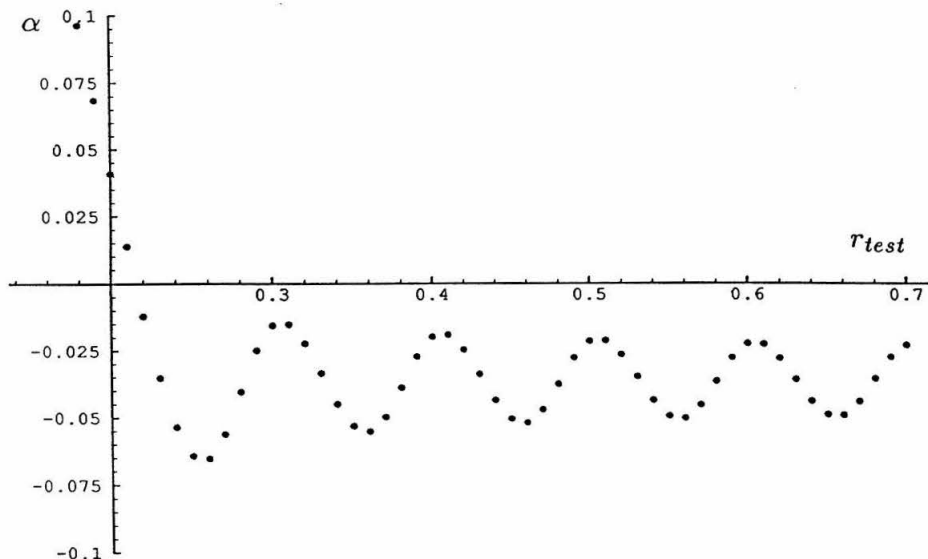


Fig. 8. The phase α as a function of where the zero area criteria is applied, *i.e.*, r_{test} .

The convergence is very fast for $n = 0$ and is apparent above one wavelength of the oscillation (as for Bessel functions). Fig. 8 shows the values of α calculated for increasing values of r_{test} . The oscillation at (twice) the frequency of the oscillating part of the asymptotic wavefunction is observed. Increasing the value of m ; the number of points in the area sum, shows that the upper peaks of the oscillations are more stable than the lower. The troughs decrease in depth for increasing m although

they do not disappear in the $m \rightarrow \infty$ limit, because the subleading r behaviour is being probed. The height of the oscillations should go to zero for $r \rightarrow \infty$ in the $m \rightarrow \infty$ limit. This can be seen to be occurring.

Fitting a $1/r_{test}$ curve to upper peaks the $r_{test} \rightarrow \infty$ limit is evaluated and the height of the amplitude of the oscillations is taken to be the error bar. Table 5 shows the values of α obtained for various values of k_1^2 (for $m = 10$ and enough significant figures and high enough powers of r to get convergence as r_{test} is increased), and compares them to the predicted values of March-Russell *et al.* Values consistent with zero are obtained over four magnitudes of the small parameter k_2^4/Γ^2 .

| | (M-RPW) | $k_1^2 = -99000$ | $k_1^2 = -9000$ | $k_1^2 = -2000$ | $k_1^2 = -40$ |
|-------------------------|-----------------|---------------------|-----------------|-----------------|----------------|
| k_2^4/Γ^2 | $\rightarrow 0$ | $\frac{1}{10\,000}$ | $\frac{1}{100}$ | $\frac{1}{9}$ | 0.92 |
| <i>max</i> | | 302 | 142 | 102 | 162 |
| $n \setminus$ sig. fig. | | 50 | 30 | 35 | 30 |
| 0 | -.207 | $-.107 \pm .04$ | $-.07 \pm .02$ | $-.035 \pm .02$ | $.04 \pm .02$ |
| 1 | -.081 | | $-.05 \pm .02$ | $-.02 \pm .02$ | $.04 \pm .02$ |
| 2 | -.050 | | $-.007 \pm .02$ | $-.006 \pm .02$ | $.005 \pm .02$ |
| 3 | -.036 | | | $-.005 \pm .02$ | $.01 \pm .02$ |
| 4 | -.028 | | | | $.006 \pm .04$ |
| 5 | -.023 | | | | $.007 \pm .06$ |
| 6 | -.019 | | | | $-.03 \pm .08$ |

Table 5. Values of α ; the difference to pure Aharonov-Bohm phase shifts.

Thus the numerical results are consistent with the phases predicted by the analytical analysis of this thesis and not with that of March-Russell *et al.*

APPENDIX 3A

3A1 SOLVING THE PARTIAL DIFFERENTIAL EQUATION FOR $T(t)$.

If $\Phi(r) = r^{k_0} \int_a^b T(t) e^{irt} dt$ solves the differential equation that we are interested in: $\nabla_n \Phi = 0$, then it must be a solution to the equation

$$\tilde{a}tT + \frac{\partial}{\partial t}(\tilde{b} + \tilde{c}t^2)T + \frac{\partial^2}{\partial t^2}(\tilde{d}t + \tilde{e}t^3)T - \frac{\partial^3}{\partial t^3}(t^2 - A^2)(t^2 - B^2)T = 0, \quad (3A1)$$

where

$$\begin{aligned} \tilde{a} &= (2k_0 + 1)(2k_0 + 1 + 2[k_0^2 - \nu_n^2]) \\ \tilde{b} &= (k_0^2 - \nu_n^2 + 2k_0 + 2)(2\omega^2 - \mu_1^2 - \mu_2^2) + (2k_0 + 2)(\mu_1^2 - \mu_2^2) \\ \tilde{c} &= 2\nu_n^2 - 6k_0^2 - 12k_0 - 7 \\ \tilde{d} &= -(2k_0 + 3)(2\omega^2 - \mu_1^2 - \mu_2^2) - 2(\mu_1^2 - \mu_2^2) \\ \tilde{e} &= 4k_0 + 6. \end{aligned} \quad (3A2)$$

or equivalently

$$atT + (b + ct^2)T' + (dt + et^3)T'' - (t^2 - \omega^2 + \mu_1^2)(t^2 - \omega^2 + \mu_2^2)T''' = 0, \quad (3A3)$$

where

$$\begin{aligned} a &= (1 - 2k_0)(2k_0 - 1 - 2[k_0^2 - \nu_n^2]) \\ b &= (k_0^2 - \nu_n^2 - 2k_0 + 2)(2\omega^2 - \mu_1^2 - \mu_2^2) + (2k_0 - 2)(\mu_1^2 - \mu_2^2) \\ c &= 2\nu_n^2 - 6k_0^2 + 12k_0 - 7 \\ d &= -(2k_0 - 3)(2\omega^2 - \mu_1^2 - \mu_2^2) - 2(\mu_1^2 - \mu_2^2) \\ e &= 4k_0 - 6, \end{aligned} \quad (3A4)$$

and $A = \pm\sqrt{\omega^2 - \mu_1^2}$, and $B = \pm\sqrt{\omega^2 - \mu_2^2}$.

$T(t)$ appears to be third order. However, it is not: it is only second order and the formula can be recast into a particularly simple form although it is still too difficult to solve.

Note that

$$\tilde{a} = \begin{cases} 0 & \text{for } k_0 = k_0^{(-)} = n : n \geq 0; \\ 4n(2n - 1) & \text{for } k_0 = k_0^{(-)} = -n : n \leq 0; \\ 4(n + 1)(2n + 3) & \text{for } k_0 = k_0^{(+)} = (n + 1) : n \geq -1; \\ 0 & \text{for } k_0 = k_0^{(+)} = -(n + 1) : n \leq -1, \end{cases} \quad (3A5)$$

and compare to the first coefficient in the other form of the equation

$$a = \begin{cases} -4n(2n - 1) & \text{for } k_0 = k_0^{(-)} = n : n \geq 0; \\ 0 & \text{for } k_0 = k_0^{(-)} = -n : n \leq 0; \\ 0 & \text{for } k_0 = k_0^{(+)} = (n + 1) : n \geq -1; \\ -4(n + 1)(2n + 3) & \text{for } k_0 = k_0^{(+)} = -(n + 1) : n \leq -1. \end{cases} \quad (3A6)$$

Exactly opposite.

So the third order equation is reduced to two different second order ones considering only the form for which the first coefficient is zero. Now re-write these two second order equations without a first order derivative.

Firstly, for the $a = 0$ (or $k_0 = k_0^U$) regime, let $S = T'$, $\alpha = (b + ct^2)$, $\rho = (dt + et^3)$, and $X = (t^2 - A^2)(t^2 - B^2)$, then

$$\alpha S + \rho S' - X S'' = 0. \quad (3A7)$$

Then set $S = G_S \Phi$ where $\Phi'/\Phi = \rho/2X$ and

$$G_S'' = G_S \left\{ \frac{\alpha}{X} + \frac{\chi''}{\chi} \right\} \quad (3A8)$$

if $\chi = 1/\Phi$. Further α/X may be written as the derivative of a function, $\log w$,

$\alpha/X = w'/w$ and then

$$\frac{G_S''}{G_S} = \frac{\chi''}{\chi} + \frac{w'}{w}, \quad (3A9)$$

which is the final result, χ and w are known and are products of powers of the singular points.

Secondly, for $\tilde{a} = 0$ (or $k_0 = k_0^L$) we note

$$(\tilde{b} + \tilde{c}t^2)T + \frac{\partial}{\partial t}(\tilde{d}t + \tilde{e}t^3)T - \frac{\partial^2}{\partial t^2}(t^2 - A^2)(t^2 - B^2)T = \text{const.} \quad (3A10)$$

which again we re-write as

$$\tilde{\alpha}T + (\tilde{\rho}T)' - (XT)'' = -\kappa, \quad (3A11)$$

where $\tilde{\alpha} = (\tilde{b} + \tilde{c}t^2)$, and $\tilde{\rho} = (\tilde{d}t + \tilde{e}t^3)$. Then writing $T = G_T\tilde{\Phi}/X$, where $\tilde{\Phi}'/\tilde{\Phi} = \tilde{\rho}/2X$ we may re-write this equation as

$$\frac{G_T''}{G_T} = \frac{\tilde{\Phi}''}{\tilde{\Phi}} + \frac{v'}{v} + \frac{\kappa}{\tilde{\Phi}G_T}, \quad (3A12)$$

where $v'/v = \tilde{\alpha}/X$. The two equations are remarkably similar and second order for the solution generating function T .

Note that

$$\begin{aligned} \Phi &= (t^2 - A^2)^{\frac{1}{2}(k_0 - \frac{1}{2})} (t^2 - B^2)^{\frac{1}{2}(k_0 - \frac{5}{2})} \\ \tilde{\Phi} &= (t^2 - A^2)^{\frac{1}{2}(k_0 + \frac{5}{2})} (t^2 - B^2)^{\frac{1}{2}(k_0 + \frac{1}{2})}. \end{aligned} \quad (3A13)$$

and also

$$\begin{aligned} w &= \left| \frac{t-A}{t+A} \right|^{\nu_A} \left| \frac{t-B}{t+B} \right|^{\nu_B} \\ v &= \left| \frac{t-A}{t+A} \right|^{\tilde{\nu}_A} \left| \frac{t-B}{t+B} \right|^{\tilde{\nu}_B}, \end{aligned} \quad (3A14)$$

where

$$\begin{aligned}\nu_A &= \frac{b + A^2c}{2A(A^2 - B^2)} \\ \nu_B &= \frac{b + B^2c}{2B(B^2 - A^2)},\end{aligned}\tag{3A15}$$

and similarly, replace b and c by \tilde{b} and \tilde{c} for $\tilde{\nu}$. Thus all of the information in the differential equations for T , equations (3A9) and (3A12), is encoded in the four functions of equations (3A13) and (3A14).

3A2 TRIVIAL SOLUTIONS.

A descending series solutions for T may truncate at powers 0, 1 or 2, of t . In the $k_0 = k_0^L$ case we have three possible truncations for ascending series: $\mu_1 = 2k_0^L - 1$, $\mu_2 = 2k_0^L$ and $\mu_3 = -2$; two are even and one is odd. We can always find one finite series solution containing positive powers of t . To truncate at both ends a series with a recursion relation (equation (3.31) is the recursion relation for $T(t)$ coefficients in a power series expansion in t) that contains three different coefficients, three truncating powers (whose multiplying factors in the recursion relation are zero) are required, two above and one below or *vice versa*—only the even powers satisfy this condition. Thus there is a solution of the form

$$T(t) = 1 + a_2t^2 + \dots + a_{2k_0^L}t^{2k_0^L}\tag{3A16}$$

The first few are constructed in table 6. For the $k_0 = k_0^U$ case there is only one finite series solution, $T = 1$, as this leaves only two truncating powers. An even series may start at t^2 , but ensuring the correct ratio of coefficients a_2 and a_4 makes the series ascension unique but does not give the required ratio of a_{2k^U} and a_{2k^U-2} to truncate its ascent at a_{2k^U} . Further note that this solution, T_0 say, is the particular solution to equation (3A11)

$$\tilde{\alpha}T_0 + (\tilde{\rho}T_0)' - (XT_0)'' = -\kappa_0,\tag{3A17}$$

for some κ_0 and so the remaining complimentary solutions are the integrals of

$$\tilde{\alpha}T_0 + (\tilde{\rho}T_0)' - (XT_0)'' = 0, \quad (3A18)$$

thus reducing the problem to a second order differential equation also.

| $k_0 = k_0^L$ | $T(t)$ |
|---------------|---|
| 0 | $T = 1$ |
| 1 | $T = (3A^2 - 5B^2) + 4t^2$ |
| 2 | $T = (-55A^4 - 30B^2A^2 + 121B^4) + (120A^2 - 264B^2)t^2 + 96t^4$ |
| k_0 | $T = 1 + a_2t^2 + \dots + a_{2k_0^L}t^{2k_0^L}$ |

Table 6. Trivial solutions for T for $k_0 = k_0^L$.

Thus two solutions remain: one is even and one is odd and they both may have branch points.

REFERENCES

1. J. March-Russell, J. Preskill, and F. Wilczek, *Phys. Rev. Lett.* **68**, (1992).
2. G.N. Watson, "*Theory of Bessel Functions*," Cambridge, (1944).

4. Conclusions and Discussion.

The result is that the scattering of a global field off a global vortex which causes a mass splitting (of the scattered field) gives rise to a scattering cross section that is of exactly the same form as scattering by a field (an electron) off a local gauge symmetry vortex (magnetic flux tube). The equivalent local gauge symmetry is the on-diagonal part of the effective local connection that arises as a result of frame dragging around the vortex. The result of such scattering is the Aharonov-Bohm cross section.

At energies above the higher mass, there is no observable scattering if the laboratory is bigger than $R_0 = \sqrt{\Gamma}/k^2$ for a wave packet of typical momenta k . As the mass splitting is reduced to zero, the region that the vortex affects is reduced to zero.

This result must be advanced as a provocative calculation; I make no claim to rigor. Further, no explicit solution was constructed, and it may be that the branch point structure of such a function is not understood from the above naive analysis. The function $(t^2 - B^2)^{k-1/2}$ solves the third order differential equation for T to order $A^2 - B^2 = 2\Gamma$, and a perturbation expansion in this may be made—logarithmic branch point structure shows up at the branch points. However, the full solution should only have branch points of the specified orders, as a power series expansion shows—some subtlety is apparent.

Let us assume that the result is correct. It is a profound and elegant result. Obtaining the cross section of a pure gauge theory in a theory with only global symmetries is striking. March-Russell, Preskill and Wilczek^[1] point out that this is counter intuitive because gauge charges have a universal coupling strength whilst global charges do not, and thus a parameter independent cross section (they call it ‘geometric’) would not be expected to arise. The simple reason is that as the mass-splitting is switched off, the Aharonov-Bohm cross section should disappear. So the fact that the mass-splitting does not explicitly appear in the cross section is a potential cause for surprise. But the resolution is along the lines that March-Russell *et al.* speculated. The form remains the same, but the range of validity is sent to zero. There are no corrections for a laboratory experiment bigger than R_0 (perhaps

the corrections they found were just those corrections that show up as the momenta is sent to zero and hence the radius of influence goes to infinity) thus making the result more striking.

The adiabatic condition has relaxed to the regime of exciting one of the masses and not the other rather than the $\Gamma/k^2 \rightarrow 0$ limit according to March-Russell *et al.* Also, the energy must be less than the symmetry breaking scale F , of the order parameter.

$$k^2 < F^2, \quad (4.1)$$

otherwise Goldstone boson excitation (*i.e.*, exciting the λ field) will obscure the effect.

Moreover, we have a tentative indication that there may be an extension of the range of validity of the adiabatic theorem and Berry's phase. The usual treatment of adiabatic Hamiltonians is to look for a parameterised Hamiltonian in a regime where there are no gradient operators in the parameters. In the case of atomic theory and the Born-Oppenheimer approximation^{*}, the parameters are the nuclear co-ordinates R say, and in particular the direction of the dipole moment of the nucleus which affects the electron wavefunction. The adiabatic approximation amounts to dropping the nuclear kinetic terms $-\frac{\partial^2}{\partial R^2}$. But this thesis attempts an analogous adiabatic calculation without this approximation, and still a Berry's phase type result was obtained for the cross section. Note that the wavefunctions themselves are modified and so transition rates will not be the same—only the perfectly elastic scattering cross section is the same.

Perhaps the holonomy arguments may be carried through for this case and the result put on a more general footing. The case to be considered would be Hamiltonians of the form

$$H(x, \frac{\partial}{\partial x}; B, \frac{\partial}{\partial B})\Phi(B, x) = 0, \quad (4.2)$$

and the question is whether or not the transport around a degeneracy gives rise to the

* *e.g.*, see the papers by Moody, Shapere, and Wilczek^[2].

usual local gauge structure, with the degeneracy acting as a monopole in configuration space.

The correct application of the adiabatic theorem in the adiabatic limit, for this case at least, is that gradient operators should be replaced by their expectation value in the basis, *i.e.*, off-diagonal parts dropped, as Goldhaber^[3] guessed. This results in the correct asymptotic behaviour for wavefunctions, and hence cross sections are calculated correctly but not transition probabilities (*i.e.*, overlap integrals of wavefunctions).

Calculations of the monopole case and the general holonomy treatment of Berry's phase are begging. More work on this topic is certainly of interest and may be very fruitful[†]. Further generalisations of the work of March-Russell *et al.* may be considered for exotic systems exhibiting global 'Alice' strings and Cheshire charge^[5].

Lastly, a piece of wild speculation: the trick of getting a perfect local gauge symmetry from a theory only possessing global symmetries is a surprise and begs the speculation that some or all of the local gauge symmetries in nature (the forces) may be global and reveal themselves to be so at higher energies. Or, at low energies the non-pure gauge nature of the interactions might be observed. Detailed signatures of the wave functions would need to be observed, not just scattering cross sections.

[†] The monopole case would be somewhat complicated, I suspect. However, a recent preprint of Davis and Martin^[4] elucidates a case that may be much easier. They have incorrectly missed the off-diagonal terms and resulted in a coupled second order equation that gives an exactly Aharonov-Bohm cross section. This cannot be correct as the effect is indicated to not disappear; its disappearance is the central issue of the problem. The inclusion of the off-diagonal terms results in a fourth order differential equation, and the analysis will be similar and perhaps easier.

REFERENCES

1. J. March-Russell, J. Preskill, F. Wilczek, *Phys. Rev. Lett.* **68**, (1992).
2. J. Moody, A. Shapere, and F. Wilczek, *Phys. Rev. Lett.* **52**, 2111 (1984);
J. Moody, A. Shapere, and F. Wilczek, “*Geometric Phases in Physics*,” pp 160–183, Eds. A. Shapere and F. Wilczek, Singapore: World Scientific (1989).
3. A. Goldhaber, private communications with J. Preskill.
4. A. C. Davis and A. P. Martin, “*A Global Analogue of the Aharonov-Bohm Effect*,” DAMPT preprint, DAMPT 93-09 (April 1993).
5. P. McGraw, “*A Global Analogue of Cheshire Charge*,” Caltech preprint, CALT-68-1865 (May 1993).